Activation of the K_{ATP} channel by Mg-nucleotide interaction with SUR1

Peter Proks, Heidi de Wet, and Frances M. Ashcroft

Department of Physiology, Anatomy and Genetics, University of Oxford, Oxford OX1 3PT, England, UK

The mechanism of adenosine triphosphate (ATP)-sensitive potassium (K_{ATP}) channel activation by Mg-nucleotides was studied using a mutation (G334D) in the Kir6.2 subunit of the channel that renders K_{ATP} channels insensitive to nucleotide inhibition and has no apparent effect on their gating. K_{ATP} channels carrying this mutation (Kir6.2-G334D/SUR1 channels) were activated by MgATP and MgADP with an EC_{50} of 112 and 8 μM, respectively. This activation was largely suppressed by mutation of the Walker A lysines in the nucleotide-binding domains of SUR1: the remaining small (~10%), slowly developing component of MgATP activation was fully inhibited by the lipid kinase inhibitor LY294002. The EC_{50} for activation of Kir6.2-G334D/SUR1 currents by MgADP was lower than that for MgATP, and the time course of activation was faster. The poorly hydrolyzable analogue MgATPγS also activated Kir6.2-G334D/SUR1. AMPPCP both failed to activate Kir6.2-G334D/SUR1 and to prevent its activation by MgATP. Maximal stimulatory concentrations of MgATP (10 mM) and MgADP (1 mM) exerted identical effects on the single-channel kinetics: they dramatically elevated the open probability ($P_O > 0.8$), increased the mean open time and the mean burst duration, reduced the frequency and number of interburst closed states, and eliminated the short burst states. By comparing our results with those obtained for wild-type K_{ATP} channels, we conclude that the MgADP sensitivity of the wild-type K_{ATP} channel can be described quantitatively by a combination of inhibition at Kir6.2 (measured for wild-type channels in the absence of Mg^{2+}) and activation via SUR1 (determined for Kir6.2-G334D/SUR1 channels). However, this is not the case for the effects of MgATP.

INTRODUCTION

ATP-sensitive potassium (K_{ATP}) channels serve as metabolic sensors, coupling cell metabolism to plasmalemmal potassium fluxes and electrical activity in a variety of cell types (Miki and Seino, 2005; Ashcroft, 2007). Their activity is primarily determined by intracellular adenosine nucleotides, with ATP having an inhibitory effect and Mg-nucleotides (MgATP or MgADP) having a stimulatory effect on channel activity.

The β cell K_{ATP} channel is an octameric (4:4) complex of two different types of protein subunit: Kir6.2 and SUR1 (Clement et al., 1997; Mikhailov et al., 2005). Four Kir6.2 subunits form a potassium-selective, weakly inwardly rectifying pore. Each Kir6.2 subunit also bears a binding site for adenine nucleotides, and the binding of ATP or ADP to one or more of these sites leads to closure of the pore. Each Kir6.2 subunit is complexed with an SUR1 subunit, and both subunits contain ER retention signals that prevent traffic to the plasma membrane in the absence of their partner subunit. Truncation of the last 26 (or 36) residues of Kir6.2 (Kir6.2ΔC), however, deletes the ER retention signal and enables surface expression of Kir6.2 channels in the absence of SUR1 (Tucker et al., 1997).

SUR1 is a member of the ATP-binding cassette protein family (Aittoniemi et al., 2009). SUR1 endows the Kir6.2 pore with sensitivity to the stimulatory effects of nucleotides (Nichols et al., 1996; Gribble et al., 1997b, 1998) and to activation or inhibition by therapeutic drugs. In common with other ABC proteins, SUR1 contains two nucleotide-binding domains (NBDs) that are involved in the binding and hydrolysis of Mg-nucleotides. These NBDs associate in a head-to-tail fashion with the Walker A and Walker B motifs of one NBD interacting with the linker domain of the other NBD to form two composite ATP-binding sites. Occupancy of site 2 by MgADP, either by direct binding of the nucleotide or by hydrolysis from MgATP, is thought to activate the channel (Zingman et al., 2001). What happens at site 1 is less clear, but mutagenesis experiments indicate that nucleotide binding at this site is also required for channel activation and ATP hydrolysis by SUR (Nichols et al., 1996; Gribble et al., 1997b, 1998).

Metabolic regulation of the K_{ATP} channel involves both inhibition at Kir6.2 and activation via SUR1. To analyze these processes in detail, it is necessary to study them in isolation from one another. In the case of inhibition, this can be achieved by experiments in Mg-free solutions, as nucleotides do not interact with SUR1 in the absence of the cation. Consequently, there have been numerous studies of how ATP blocks the channel by binding

Correspondence to Frances M. Ashcroft: frances.ashcroft@dpag.ox.ac.uk

Abbreviations used in this paper: DAMN, decline of activation by Mg-nucleotides; K_{ATP}, ATP-sensitive potassium; NBD, nucleotide-binding domain; PKIP, PKA inhibitory peptide.

The Rockefeller University Press $30.00
J. Gen. Physiol. Vol. 136 No. 4 389–405
www.jgp.org/cgi/doi/10.1085/jgp.201010475

to Kir6.2 (for review see Proks and Ashcroft, 2009). In contrast, much less attention has been paid to how Mg-nucleotides stimulate the K_{ATP} channel because it has been difficult to isolate activation from the confounding effects of simultaneous inhibition at Kir6.2. A further complication is that nucleotide activation and inhibition may not be independent but might interact.

The first step in elucidating the mechanism of Mg-nucleotide activation is to measure its effect in the absence of inhibition at Kir6.2. This can be achieved by using a mutant Kir6.2 that is insensitive to ATP block but retains normal gating properties. To date, many mutations in Kir6.2 that strongly impair ATP inhibition have been identified, but in most cases, some block still remains at ATP concentrations >1 mM. The Kir6.2-G334D mutation stands out, as it appears to be insensitive to ATP even at very high concentrations (Drain et al., 1998; Masia et al., 2007). Residue G334 lies within the putative ATP-binding site of Kir6.2, and its mutation to aspartate is believed to prevent ATP binding electrostatically (Antcliff et al., 2005). Previous studies have shown no obvious effect of the G334D mutation on the intrinsic (i.e., unliganded) single-channel kinetics of Kir6.2ΔC26 channels (Drain et al., 1998) or the open probability of Kir6.2-G334D/SUR1 channels (Masia et al., 2007). These results make K_{ATP} channels carrying this mutation potentially suitable for studying the mechanism of nucleotide activation of the wild-type K_{ATP} channel. Here, we have used Kir6.2-G334D as a tool to quantify channel activation by Mg-nucleotides at both the macroscopic and single-channel level.

MATERIALS AND METHODS

Molecular biology

Human Kir6.2 (available from GenBank/EMBL/DDBJ under accession no. NM_000525 with E23 and I377) and rat SUR1 (available from GenBank/EMBL/DDBJ under accession no. L4_0624) were used in this study. We used rat SUR1 rather than human SUR1 because in our hands it expressed larger currents in excised patches exposed to nucleotide-free solution: we make the assumption that rat SUR1 behaves like human SUR1. Site-directed mutagenesis of SUR1 or Kir6.2, preparation of mRNA, and isolation of *Xenopus laevis* oocytes were performed as described previously (Proks et al., 2005b). Oocytes were injected with 0.8 ng of wild-type or mutant Kir6.2 mRNA and ∼4 ng of SUR1 mRNA. Currents were recorded 1–3 d after injection.

Electrophysiology

Patch electrodes were pulled from thick-walled borosilicate glass (Harvard Electronics). PIP_2 and PIP_3 antibodies were obtained from Invitrogen, and all other chemicals were from Sigma-Aldrich. Nucleotide-containing solutions were applied using a rapid solution changer (model RSC-200; Biological Science Instruments). Currents were recorded using an Axopatch 200B (Axon Instruments) and pClamp software (Axon Instruments).

All experiments were performed at room temperature (20–22°C). The pipette solution contained (in mM): 140 KCl, 1.2 $MgCl_2$, 2.6 $CaCl_2$, and 10 HEPES, pH 7.4 with KOH. In most experiments, the internal (bath) solution contained (in mM): 107 KCl, 1 $CaCl_2$, 2 $MgCl_2$, 10 EGTA, and 10 HEPES, pH 7.2 with KOH. Adenosine nucleotides were added to intracellular solution as the Mg^{2+} salt, and the pH was then readjusted with KOH. The Mg-free solution contained (in mM): 107 KCl, 1 K_2SO_4, 10 EGTA, and 10 HEPES, pH 7.2 with KOH. ATP was added as the potassium salt. Macroscopic currents were recorded from giant inside-out patches at a constant holding potential of −60 mV. Currents were filtered at 0.15 kHz and digitized at 0.5 kHz. Single-channel activity of 3–20-min duration was recorded at −60 mV, filtered at 5 kHz, and digitized at 50 kHz.

To quantify the potency of different Mg-nucleotides at activating K_{ATP} channels carrying the G334D mutation and to examine the effect of the PKA inhibitory peptide (PKIP), activation was expressed as $(I_N-I_C)/(I_0-I_C)*100$ (%), where I_N is the steady-state K_{ATP} current in the presence of the nucleotide, I_0 is the current in nucleotide-free solution immediately after patch excision (i.e., before channel rundown), and I_C is the current in nucleotide-free solution before nucleotide application.

When measuring the relationship between nucleotide concentration and channel activation, the effect of rundown was compensated for using the protocol shown in Fig. 5 B. In brief, each test nucleotide concentration [X] was interrupted by a maximal stimulatory nucleotide concentration. The latter was determined in preliminary experiments and fixed at 10 mM for MgATP and 1 mM for MgADP. The increase in current due to the application of nucleotide concentration [X] was calculated as $(I_X-I_C)/(I_{MAX}-I_C)$, where I_X is the steady-state K_{ATP} current in the presence of test nucleotide concentration [X] (measured after switching from nucleotide-free solution), I_{MAX} is the current in the presence of the maximal stimulatory nucleotide concentration, and I_C is the current in nucleotide-free solution before switching to the test solution. The relationship between nucleotide activation and nucleotide concentration (Fig. 5 C) was then fit with Eq. 1:

$$\frac{I_X - I_C}{I_{MAX} - I_C} = \frac{[X]^h}{EC_{50}{}^h + [X]^h}, \quad (1)$$

where EC_{50} is the nucleotide concentration at which activation is half-maximal, and h is the slope factor (Hill coefficient).

The relationship between nucleotide concentration and inhibition of the wild-type K_{ATP} current in Mg-free solutions (Fig. 10) was fit with Eq. 2:

$$\frac{I_X}{I_C} = \frac{1}{1+(\frac{[X]}{IC_{50}})^h}, \quad (2)$$

where I_X is the steady-state K_{ATP} current in the presence of test nucleotide concentration [X], I_C is the current in nucleotide-free solution obtained by averaging the current before and after application of the nucleotide, IC_{50} is the nucleotide concentration at which the inhibition is half-maximal, and h is the Hill coefficient.

The concentration–response curve for Mg-nucleotide action of the wild-type K_{ATP} channel shown in Fig. 10 was fit with the product of two Hill equations, one for activation and one for inhibition (Eq. 3):

$$\frac{I_X}{I_C} = \frac{1}{1+(\frac{[X]}{IC_{50}})^{h_1}} * \frac{1+a*(\frac{[X]}{EC_{50}})^{h_2}}{1+(\frac{[X]}{EC_{50}})^{h_2}}, \quad (3)$$

where I_X is the steady-state K_{ATP} current in the presence of the test nucleotide concentration [X], I_C is the current in nucleotide-free solution (obtained by averaging the current before and after

application of the nucleotide), a is the maximal increase in K_{ATP} current (produced by Mg-nucleotide activation) expressed as a fraction of I_C, IC_{50} is the nucleotide concentration at which the inhibitory effect is half-maximal, EC_{50} is the nucleotide concentration at which the stimulatory effect is half-maximal, and h_1 and h_2 are the Hill coefficients for inhibition and activation, respectively.

For noise analysis, macroscopic currents were recorded at −60 mV, sampled at 20 kHz, and filtered at 5 kHz with an eight-pole Bessel filter. Unless blocked by ATP, K_{ATP} channels have mean open times >1 ms (see Figs. 3, 8, and 9). Thus, our conditions for data acquisition should not introduce substantial errors into our estimates of P_O and N (Silberberg and Magleby, 1993). The macroscopic mean current (I) and variance (σ) were determined from data segments of 1-s duration (see Fig. 1). Control data were taken immediately before nucleotide application and test data once a steady-state condition was reached. P_O and N were calculated according to the following equations:

$$P_O = \frac{I * i - \sigma^2}{I * i} \tag{4}$$

$$N = \frac{I^2}{I * i - \sigma^2} \tag{5}$$

Single-channel amplitude at −60 mV (i) was taken as 4 pA (Proks et al., 2001).

To examine the effect of the duration of the measurement period on P_O and N, we simulated K_{ATP} currents using the program QuB (Qin et al., 1989) for $n = 100$ and $n = 1{,}000$ using the recording conditions given above and the kinetic scheme below (Gillis et al., 1989; Furukawa et al., 1993; Alekseev et al., 1998):

$$C_F \underset{b}{\overset{a}{\rightleftharpoons}} O \underset{d}{\overset{c}{\rightleftharpoons}} C_{S1} \underset{f}{\overset{e}{\rightleftharpoons}} C_{S2}$$

(SCHEME 1)

where O is the open state, C_F is the short intraburst closed state, and C_{S1} and C_{S2} are long interburst closed states: a = 2,500 s^{-1}, b = 500 s^{-1}, d = 100 s^{-1}, and f = 10 s^{-1}. Values for c and e were calculated from P_O and the mean burst duration (τ_B), where

$$\tau_B = \frac{1 + \frac{a}{b}}{c} \tag{6}$$

$$P_O = \frac{1}{1 + \frac{a}{b} + \frac{c}{d} + \frac{c * e}{d * f}} \tag{7}$$

P_O and τ_B were varied between 0.4–0.86 and 10-1,000 ms, respectively. A good agreement between the simulated and the calculated values of P_O and N was observed for time periods ≥1 s. For intervals <1 s, the values of P_O calculated using Eq. 4 became significantly larger than those used in simulations.

Single-channel data were analyzed using a combination of Clampfit (OriginLab) and in-house software. Dwell-time histograms were constructed and analyzed at a resolution of 0.15 ms, as described previously (Davies et al., 1992). Open time distributions were fit with a single exponential; up to three exponentials were fitted to distributions of burst durations, and up to four exponentials were fitted to closed dwell-time distributions. The mean open time (τ_O) was corrected for missed events ($\tau_{O,COR}$), as described previously (Proks et al., 2001). Burst durations were determined using the criterion for the critical time described by Magleby and Pallotta (1983):

$$a_f e^{-t_{crit}/\tau_f} = \sum_{i=1}^{n} a_{si}(1 - e^{-t_{crit}/\tau_{si}}), \tag{8}$$

where a_f and τ_f are the area and mean lifetime of the intraburst state, and a_{si} and τ_{si} are the area and mean lifetime of the interburst state i (i = 1 to n).

Single-channel kinetics were analyzed in patches that showed stationary kinetics in nucleotide-free solution over a 10-min period. It is important to point out that not all channels showed this degree of stability. In ∼50% of recordings, the activatory effect of MgADP (and MgATP) was substantially impaired. Furthermore, the extent of activation was sometimes not constant but decreased during the application of the nucleotide (as found for macropatches).

Statistics

All values are given as mean ± SEM. Statistical significance was determined using Student's t test.

RESULTS

The goal of this study was to obtain a quantitative description of K_{ATP} channel activation by Mg-nucleotides. Two criteria are needed to achieve this aim. First, it is essential to remove nucleotide inhibition at Kir6.2 so that activation can be studied in isolation. Second, it is necessary to determine a reliable way of measuring activation.

Nucleotide inhibition of the K_{ATP} channel is mediated by binding to Kir6.2 (Tucker et al., 1997). Thus, we exploited the fact that the Kir6.2-G334D mutation abolishes channel inhibition completely, without affecting the single-channel kinetics in the absence of nucleotide (Drain et al., 1998; Masia et al., 2007), to quantify the properties of activation. We make the assumption

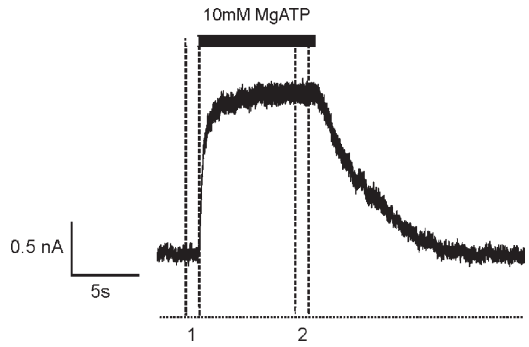

Figure 1. Data segments used for noise analysis of macroscopic Kir6.2-G334D/SUR1 currents. Representative example of activation of Kir6.2-G334D/SUR1 channels by 10 mM MgATP. Nucleotide application is indicated by the bar. The parallel vertical lines denote 1-s data segments during which the current reaches a quasi–steady-state level. The dotted horizontal line indicates the zero current level. P_O and N in the absence of nucleotides (open triangles in Fig. 4, B–D) were calculated from segment 1, and in the presence of 10 mM MgATP (open circles in Fig. 4, B–D) from segment 2.

that this mutation does not affect channel activation by SUR1.

Two phenomena complicate measurements of channel activation: (1) the rundown in channel activity (Findlay and Dunne, 1986) and (2) the decline in nucleotide activation observed after excision of inside-out patches and exposure to nucleotide-free solution (Bokvist et al., 1991). We next explore whether these processes are altered by the G334D mutation and consider how their effects may be minimized.

Rundown of Kir6.2/SUR1 and Kir6.2-G334D/SUR1 channel activity in excised patches

A common feature of K_{ATP} channels is that they show a time-dependent decline of channel activity after patch excision into nucleotide-free solution. This rundown imposes two problems on quantification of channel activation. First, it is necessary to ensure that channel activity is as stable as possible throughout the period during which channel activation is measured, and that corrections are made for any time-dependent rundown that is present. Second, rundown will influence the capacity for channel activation. As the channel open probability can never be greater than unity, the apparent magnitude of maximal activation may be less for channels with high P_O than low P_O, even when the actual activation capacity is identical.

Fig. 2 compares the behavior of Kir6.2/SUR1 and Kir6.2-G334D/SUR1 channels expressed in *Xenopus* oocytes before and after excision into nucleotide-free solution. Before excision there is little detectable Kir6.2/SUR1 current as the channels are almost completely closed by the high intracellular ATP concentration ($[ATP]_i$) found in the oocyte (Gribble et al., 1997a). Formation of an inside-out patch is followed by a rapid increase in current as ATP block is relieved by washout of adenosine nucleotides from the cytosolic side of the membrane. However, the current almost immediately starts to decline (Fig. 2 A).

In contrast to wild-type channels, Kir6.2-G334D/SUR1 channels are highly active in the cell-attached configuration, and there is usually only a small increase in current after patch excision (Fig. 2 B). This is because the G334D mutation almost completely abolishes the inhibitory effect of ATP (Drain et al., 1998; Markworth et al., 2000). In two thirds of patches (24/36), Kir6.2-G334D/SUR1 currents remained relatively stable after patch excision into nucleotide-free solution (declining <5%), provided that the intracellular solution was not perfused; however, perfusion induced an immediate and dramatic rundown of current (see Fig. 2 B for an example). In the other 30% of patches (12/36), Kir6.2-G334D/SUR1 currents declined gradually after excision, even when the solution was not perfused, but rundown was accelerated when perfusion was initiated (e.g., see Fig. 5 B).

For both types of K_{ATP} channel, once perfusion was initiated, the rate and extent of rundown varied dramatically between patches. To determine whether rundown is influenced by the G334D mutation, we compared its time course for Kir6.2/SUR1 and Kir6.2-G334D/SUR1 currents during the first 60 s of current decline (Fig. 2 C).

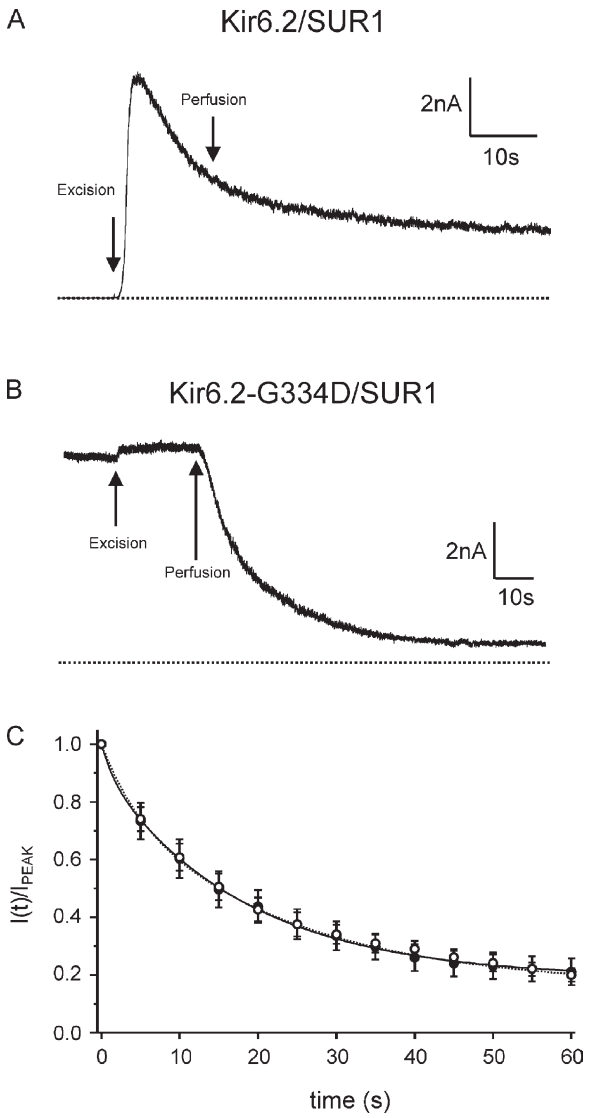

Figure 2. Rundown of Kir6.2/SUR1 and Kir6.2-G334D/SUR1 channels in macropatches. (A) Macroscopic Kir6.2/SUR1 currents at −60 mV recorded from a giant patch. Patch excision and the start of the perfusion with nucleotide-free intracellular solution are indicated by the arrows. The dotted line represents the zero current level. (B) Macroscopic Kir6.2-G334D/SUR1 currents recorded at −60 mV. Patch excision and the start of the perfusion with nucleotide-free solution are indicated by the arrows. The dotted line represents the zero current level. (C) Mean macroscopic K_{ATP} current at −60 mV during the first 60 s of rundown, expressed as a fraction of the maximum value reached after excision, is plotted as a function of the time after patch excision for Kir6.2/SUR1 (open circles; $n = 10$) and Kir6.2-G334D/SUR1 channels (filled circles; $n = 10$). The lines are the best fit of a double-exponential function to the mean data (solid line, Kir6.2/SUR1; dotted line, Kir6.2-G334D/SUR1).

TABLE I

Single-channel parameters of wild-type and Kir6.2-G334D/SUR1 channels in nucleotide-free solution

Channel	$P_O(0)$	τ_O	$\tau_{O,COR}$	τ_{B1}	a_{B1}	τ_{B2}	a_{B2}	τ_{B3}	a_{B3}	τ_B
		ms	*ms*	*ms*		*ms*		*ms*		*ms*
Wild-type	0.37 ± 0.07	2.9 ± 0.3	2.1 ± 0.2	77 ± 19	0.55 ± 0.05	28 ± 6	0.30 ± 0.04	1.4 ± 0.6	0.12 ± 0.01	52 ± 11
Kir6.2-G334D/SUR1	0.34 ± 0.04	2.8 ± 0.3	1.9 ± 0.2	63 ± 10	0.69 ± 0.08	17 ± 5	0.21 ± 0.06	1.2 ± 0.4	0.13 ± 0.02	45 ± 5

$P_O(0)$, intrinsic (ligand-free) single-channel open probability; τ_O, mean open time; $\tau_{O,COR}$, mean open time corrected for missed events (Proks et al., 2001); τ_{Bi} and a_{Bi}, burst durations and their corresponding amplitudes in the distribution of burst lengths (i =1–3); τ_B, mean burst duration. Data are expressed as mean ± SEM (n = 3 each).

In both cases, the decline in current was well fit with the sum of two exponentials and an offset value of 0.17, which represents the steady-state value of the rundown current at 60 s. There was no significant difference in the time constants and amplitudes of the two exponentials between Kir6.2/SUR1 and Kir6.2-G334D/SUR1 channels. The time constant of the fast component was 2.4 ± 1.1 s (amplitude 13 ± 3%; n = 10) for wild-type and 4.4 ± 1.2 s (amplitude 19 ± 4%; n = 10) for Kir6.2-G334D/SUR1 channels. The time constant of the slow component was 20 ± 1 s (amplitude 70 ± 2%; n = 10) for wild-type and 22 ± 1 s (amplitude 64 ± 4%; n = 10) for Kir6.2-G334D/SUR1 channels.

The similarity in the time course and extent of rundown found for Kir6.2/SUR1 and Kir6.2-G334D/SUR1 channels suggest that the mutation does not influence rundown. The data also suggest that activation is best examined at least 30 s after patch excision, when the fast component of rundown is largely complete.

We next determined if the intrinsic single-channel kinetics (i.e., those in the absence of added Mg-nucleotides) were similar in wild-type and mutant channels. Rundown of channel activity was also observed at the single-channel level. However, in some recordings, single-channel activity reached a quasi–steady state within ∼30 s and remained stable for up to ∼10 min, which enabled analysis of the channel kinetics. There was no difference between the mean open probability ($P_O(0)$) of Kir6.2/SUR1 (0.43 ± 0.05; n = 6) and Kir6.2-G334D/SUR1 (0.41 ± 0.06; n = 6) channels when measured in quasi–steady-state conditions in nucleotide-free solutions. A similar finding was reported previously (Masia et al., 2007). In addition, there were no obvious qualitative differences in channel kinetics (Fig. 3). Both wild-type and mutant channels exhibited one open state, one short intraburst state, three to four long interburst states, and three burst components (Fig. 3, B and D, and Tables I and II).

Collectively, we conclude that the G334D mutation has no effect on the rundown or intrinsic gating of K_{ATP} channels; thus, channels with this mutation constitute a reasonable model for studying the mechanism by which Mg-nucleotides activate the K_{ATP} channel.

There are several possible explanations for the marked difference in the behavior of Kir6.2/SUR1 and Kir6.2-G334D/SUR1 channels during the period between patch excision and the start of the perfusion. For example, the high activity of Kir6.2-G334D/SUR1 channels after patch excision might be maintained by agents (such as PIP_2) that bind more tightly to the mutant channel and require more vigorous perfusion to remove. It is known that PIP_2 binding to wild-type K_{ATP} channels is antagonized by ATP (Fan and Makielski, 1997); thus, if ATP binding is reduced, PIP_2 binding may be facilitated.

Decline of the activatory effect of Mg-nucleotides in excised patches

As shown in Fig. 4 A, the maximal extent of Kir6.2-G334D/SUR1 channel activation by MgATP (at 10 mM) gradually declined with repetitive applications: a similar decline was also observed for MgADP (not depicted). It has also been reported for wild-type K_{ATP} channels (Bokvist et al., 1991). To distinguish the decrease of channel activity in nucleotide-free solutions (rundown) from the decline of the activatory effect of Mg-nucleotides in excised patches, we term the latter "decline of activation by Mg-nucleotides" (DAMN).

To determine if rundown and DAMN affect the number of functional channels (N), the open probability

TABLE II

Single-channel parameters of wild-type and Kir6.2-G334D/SUR1 channels in nucleotide-free solution

Channel	τ_{C1}	a_{C1}	τ_{C2}	a_{C2}	τ_{C3}	a_{C3}	τ_{C4}	a_{C4}
	ms		*ms*		*ms*		*ms*	
Wild-type	0.40 ± 0.02	0.923 ± 0.014	15.2 ± 3.3	0.025 ± 0.003	114 ± 41	0.045 ± 0.014	253 ± 55	0.007 ± 0.002
Kir6.2-G334D/SUR1	0.40 ± 0.02	0.943 ± 0.024	12.5 ± 2.4	0.019 ± 0.007	72 ± 34	0.026 ± 0.008	299 ± 88	0.010 ± 0.004

τ_{Ci}, a_i, closed times and their corresponding amplitudes in the distribution of closed times (i =1–4). Data are expressed as mean ± SEM (n = 3 each).

(P_O), or both, we used stationary noise analysis. We analyzed the effects of a maximal stimulatory concentration of 10 mM MgATP or 1 mM MgADP for six successive nucleotide applications applied at 30-s intervals. A representative experiment is shown in Fig. 4 A. Currents in the presence of Mg-nucleotide were measured at steady state over a 1-s interval, and control currents were measured for the same time interval immediately before nucleotide application (see Fig. 1). Channel activity (NP_O; Fig. 4 B) and N (Fig. 4 D) were expressed as a fraction of that measured immediately after patch excision (for further details refer to Materials and methods).

As previously shown for wild-type K_{ATP} channels (Proks and Ashcroft, 1993), rundown of Kir6.2-G334D/SUR1 channels in nucleotide-free solution was accompanied by a decrease in both P_O (to ~0.4; Fig. 4 C) and N (to ~30% of its initial value; Fig. 4 D). Although P_O appeared to stabilize within ~30 s, N took longer to reach a steady state (Fig. 4, C and D), suggesting that they may be influenced by separate processes. Data obtained in the absence of nucleotide provide an approximation of how N and P_O change during rundown, but it should not be forgotten that rundown may be affected by the applied pulses of nucleotide.

The application of 1 mM MgADP or 10 mM MgATP increased both P_O and N, but the potency of this effect declined with successive applications (Fig. 4, B–D). Interestingly, the number of functional channels that could be reactivated appeared to decrease faster (to ~65% after six trials) than the decline in P_O (to ~75%). These data show that Mg-nucleotide activation declines with time for

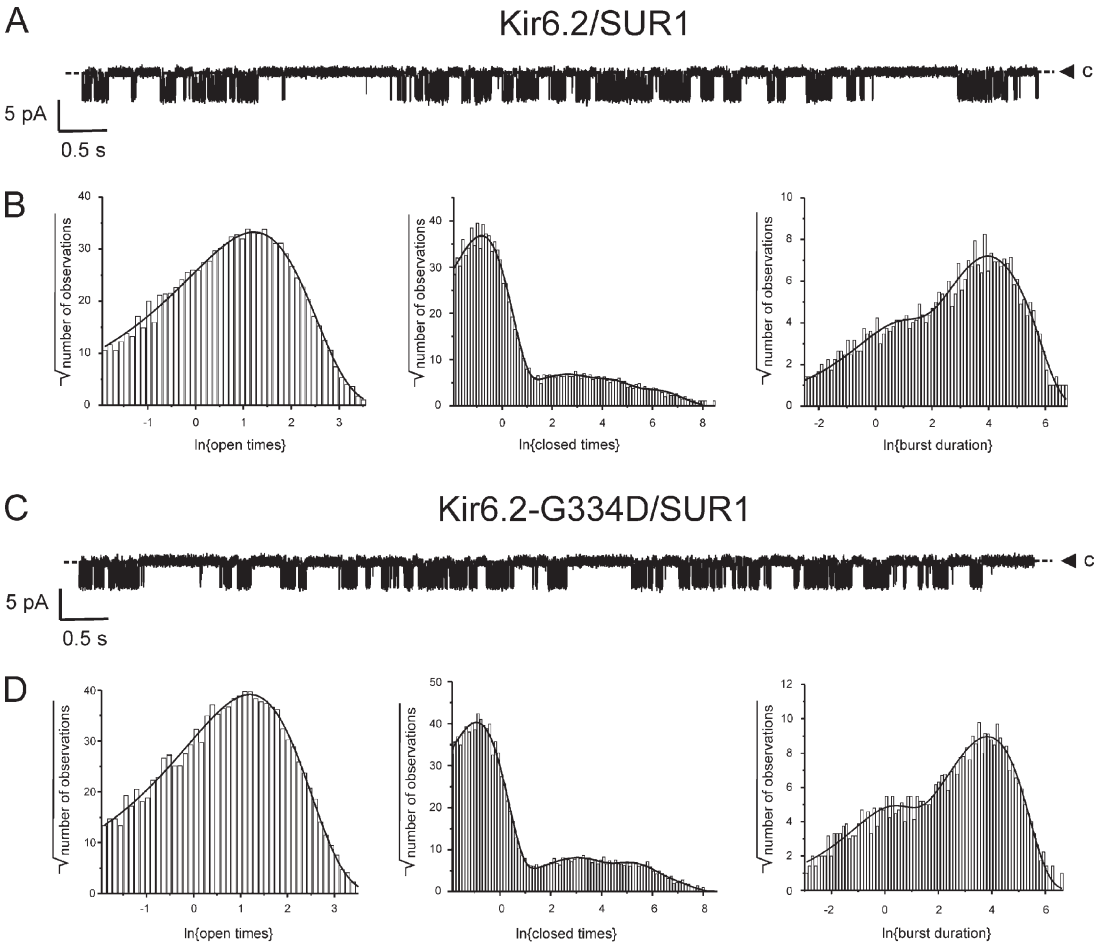

Figure 3. Kinetics of Kir6.2/SUR1 and Kir6.2-G334D/SUR1 channels. (A) Single Kir6.2/SUR1 currents recorded at −60 mV in nucleotide-free solution. c, the closed current level. (B) Distributions of Kir6.2/SUR1 open times (left), closed times (middle), and burst times (right) in nucleotide-free solution. The $P_O(0)$ of the channel illustrated was 0.36. The distributions were fit with the following parameters. Open times: τ_O = 3.39 ms ($\tau_{O,COR}$ = 2.46 ms); closed times: τ_{C1} = 0.44 ms, a_{C1} = 0.949; τ_{C2} = 9.6 ms, a_{C2} = 0.022; τ_{C3} = 53 ms, a_{C3} = 0.020; τ_{C4} = 363 ms, a_{C4} = 0.009; burst times: τ_{B1} = 93 ms, a_{B1} = 0.526, τ_{B2} = 31 ms, a_{B2} = 0.328, τ_{B3} = 1.7 ms, a_{B3} = 0.145. The mean burst duration (τ_B) was 59.3 ms. (C) Single Kir6.2-G334D/SUR1 currents recorded at −60 mV in nucleotide-free solution. c, the closed current level. (D) Distributions of Kir6.2-G334D/SUR1 open times (left), closed times (middle), and burst times (right) in nucleotide-free solution. The $P_O(0)$ of the channel illustrated was 0.27. The distributions were fit with the following parameters. Open times: τ_O = 3.32 ms ($\tau_{O,COR}$ = 2.32 ms); closed times: τ_{C1} = 0.39 ms, a_{C1} = 0.940; τ_{C2} = 16.9 ms, a_{C2} = 0.030; τ_{C3} = 139 ms, a_{C3} = 0.023; τ_{C4} = 415 ms, a_{C4} = 0.007; burst times: τ_{B1} = 61 ms, a_1 = 0.651; τ_{B2} = 20 ms, a_2 = 0.187; τ_{B3} = 1.0 ms, a_3 = 0.162. The mean burst duration (τ_B) was 43.6 ms.

Kir6.2-G334D channels, as it does for wild-type channels (Bokvist et al., 1991); thus, this must be taken into account when constructing concentration–response curves for channel activation by Mg-nucleotides.

Activation by MgADP and MgATP

The results presented above show that to reliably quantify Kir6.2-G334D/SUR1 channel activation by Mg-nucleotides, it is necessary to correct for both rundown and for the decline in the stimulatory effect of Mg-nucleotide that occurs after patch excision. This was achieved as shown in Fig. 5 B. Each test nucleotide concentration was interrupted by the maximal stimulatory concentration of the nucleotide. Channel activation was then defined as the ratio $(I_X - I_C)/(I_{MAX} - I_C)$, where I_{MAX} is the K_{ATP} current at the maximal stimulatory nucleotide concentration, I_X is the K_{ATP} current in the presence of the test nucleotide concentration ([X]), and I_C is the K_{ATP} current in the absence of the nucleotide (refer to Materials and methods for further details).

Mean concentration–activation relationships are shown in Fig. 5 C. The potency of MgADP (EC_{50} = 8 ± 3 μM; n = 8) appears to be >10-fold that of MgATP (EC_{50} = 112 ± 11 μM; n = 8). The Hill coefficients for both curves are slightly higher than unity (~1.3), indicating that the binding and cooperative interaction of more than one nucleotide molecule per K_{ATP} channel is necessary for channel activation. The EC_{50} for MgATP is similar to that previously obtained for Kir6.2-G334D/SUR1 channels (183 μM) (Masia et al., 2007), using a different expression system and no correction for DAMN.

Kinetics of Mg-nucleotide activation and deactivation

At a concentration of 1mM, MgADP and MgATP were equally potent at activating Kir6.2-G334D/SUR1 (Fig. 6 A). However, two exponential components were always required to fit the time course of MgATP activation, whereas in most experiments (9 out of 13) the time course of MgADP activation was well fit with a single exponential (Fig. 6, B and C). Furthermore, the fast on-rate and the off-rate were significantly faster for MgADP than for MgATP (Fig. 6, B and C). Although the off-rate for MgADP might be limited by the rapidity of the solution change, the slower off-rate of MgATP must reflect the time required for ATP hydrolysis and/or Pi unbinding. In all cases, the off-rates were slower than the fast on-rate.

Effects of nonhydrolyzable adenosine nucleotides

According to the current consensus view, MgATP has to be hydrolyzed to MgADP by the NBDs of SUR to stimulate channel activity (Zingman et al., 2001). Interestingly, the poorly hydrolyzable ATP analogue MgATPγS (1 mM) was as effective as MgATP at stimulating the activity of Kir6.2-G334D/SUR1 channels (Fig. 6 A). In both cases, the time course of channel activation was well fit with the sum of two exponentials, whereas a single exponential was sufficient to fit the time course of deactivation

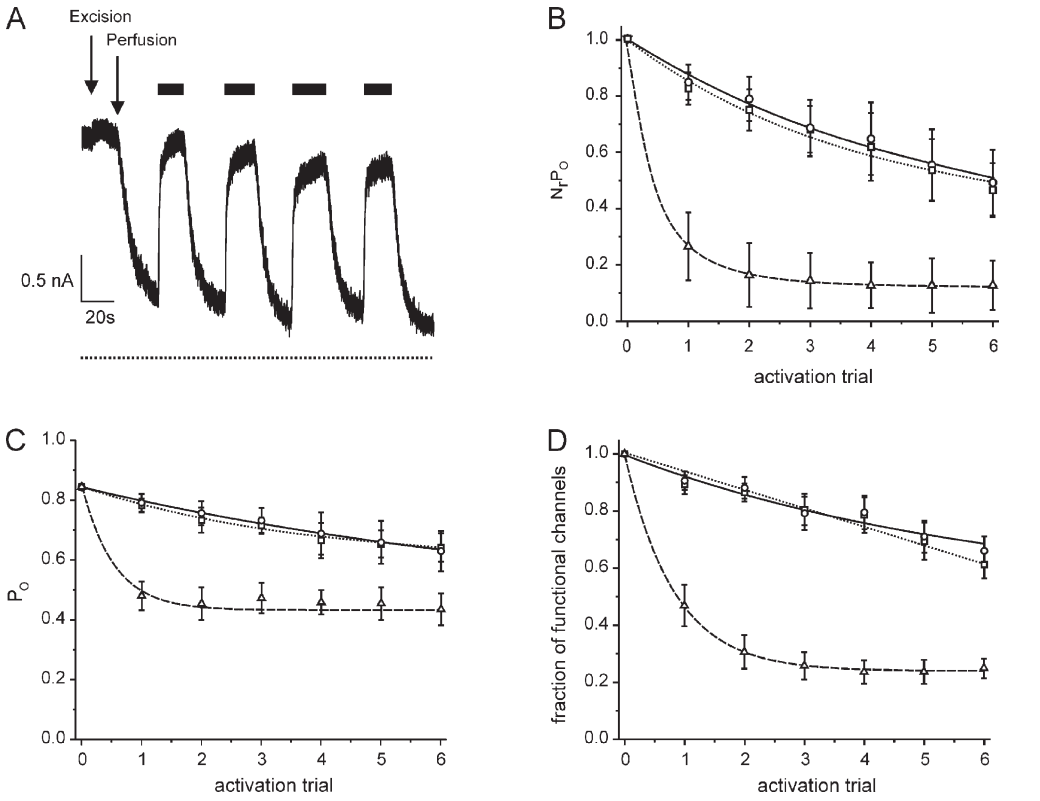

Figure 4. Rundown and reactivation of Kir6.2-G334D/SUR1 channels by MgATP and MgADP. (A) Representative record showing repetitive activation of Kir6.2-G334D/SUR1 current by 10 mM MgATP. Nucleotide application is indicated by the bars. Patch excision and the start of the perfusion with nucleotide-free solution are indicated by the arrows. The dotted line indicates the zero current level. (B–D) Estimates of N_rP_O (B), P_O (C), and the fraction of functional channels (N) (D) calculated from noise analysis of current records obtained during repetitive application of 10 mM MgATP (open circles) or 1 mM MgADP (open squares), or in control solution before the application of nucleotide (open triangles). Data are mean ± SEM from 10 patches. The lines are drawn by eye.

on return to nucleotide-free solution. The mean on-rates and off-rates for MgATPγS activation were only slightly slower than those of MgATP (Fig. 6 B), suggesting that any differences in the rate of hydrolysis are small or that other steps in the activation process are rate-limiting.

In contrast to MgATPγS, the application of the non-hydrolyzable analogue MgAMP-PNP (1 mM) to the intracellular membrane surface produced only a tiny (~5%) increase in Kir6.2-G334D/SUR1 current, which did not reach significance (Fig. 6 A). Furthermore, MgAMP-PNP did not impair the activatory effect of 1 mM ATP, suggesting that it does not compete with ATP for the nucleotide-binding sites on SUR1. This argues that MgAMP-PNP binds poorly to SUR1.

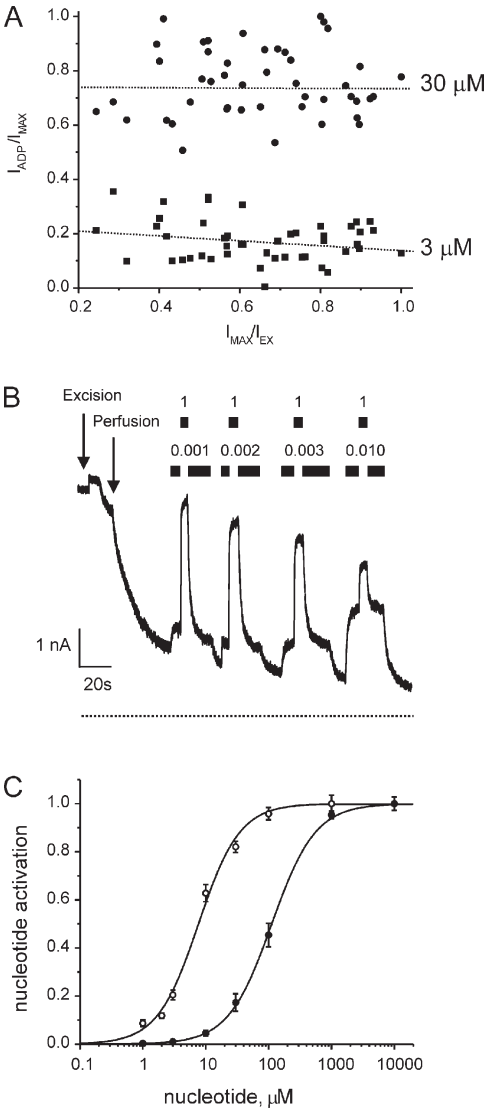

Figure 5. Nucleotide activation of Kir6.2-G334D/SUR1 channels. (A) Kir6.2-G334D/SUR1 current magnitude (I_{ADP}) in the presence of 3 μM MgADP (filled squares) or 30 μM MgADP (filled circles), expressed as a fraction of that in the presence of a maximal stimulatory ADP concentration (1 mM; I_{MAX}). This is plotted against the current magnitude in the presence of 1 mM MgADP (I_{MAX}), expressed as a fraction of the current immediately after excision (I_{EX}). The dotted lines represent the best linear fit to the data at 3 μM (lower) or 30 μM (upper) MgADP. (B) Repetitive activation of Kir6.2-G334D/SUR1 channels by different concentrations of MgADP. Nucleotide application is indicated by the bars, and the numbers above the bars give the nucleotide concentration in millimolars. The dotted line indicates the zero current level. (C) Concentration–response relationships for activation of Kir6.2-G334D/SUR1 channels by MgATP (filled circles; $n = 8$) or MgADP (open circles; $n = 8$). The lines are the best fit of Eq. 1 to the mean data with $EC_{50} = 7.7$ μM and $h = 1.30$ (MgADP) and $EC_{50} = 112$ μM and $h = 1.25$ (MgATP).

Mg-nucleotide activation in the absence of functional NBDs of SUR1

Previous studies have shown that the activatory effect of Mg-nucleotides is mediated by the NBDs of SUR1 and is abolished by mutation of residues in the Walker A, Walker B, or linker motifs of the NBDs (Gribble et al., 1997b; Shyng et al., 1997). To confirm that this is also the case for Kir6.2-G334D/SUR1 channels, we mutated the Walker A lysine in both NBD1 and NBD2 to alanine (SUR1-KAKA) and examined the effects of a maximally effective concentration of Mg-nucleotide.

As shown in Fig. 7 A, the application of 1 mM MgATP elicited a small, slowly developing increase in Kir6.2-G334D/SUR1-KAKA current. The mean steady-state value of this increase was 8.8 ± 0.2% ($n = 10$). To determine if this increase was mediated via Kir6.2 or SUR1, we tested the effect of 1 mM MgATP on a truncated Kir6.2 subunit containing the G334D mutation (Kir6.2-G334DΔC), expressed in the absence of SUR1 (Fig. 7 B). The mean current increase was 7.8 ± 0.9% ($n = 8$), not significantly different from that observed for Kir6.2-G334D/SUR1-KAKA channels. This suggests that the slow increase seen for Kir6.2-G334D/SUR1-KAKA channels does not involve SUR1 but is intrinsic to Kir6.2.

A possible explanation for the residual activation by MgATP is that it is due to MgATP-generated PIP_2, which is well established to stimulate the K_{ATP} channel (Baukrowitz et al., 1998; Shyng and Nichols, 1998). A similar idea has been advanced for wild-type K_{ATP} channels (Xie et al., 1999). To test this hypothesis, we used 0.1 mM LY294002 to inhibit both PI3 kinase (IC_{50} = 1.5 μM) and PI4 kinase (IC_{50} = 34 μM), which generate PIP_2 (Rosado and Sage, 2000). In the absence of nucleotide, LY294002 had no immediate effect on Kir6.2-G334D/SUR1-KAKA channels but completely abolished the stimulatory effect of 1 mM MgATP (mean current increase 0.1 ± 0.1% vs. 5.4 ± 0.1% for control, measured in the same patch; $n = 5$). The application of a PIP_2 antibody (15 μg/ml), however, was without effect on Kir6.2-G334D/SUR1-KAKA activation (increase 8.6 ± 0.3% vs. 8.2 ± 0.3% for control; $n = 5$). A similar result was obtained with a PIP_3 antibody ($n = 5$; not depicted). Thus, it is not clear whether PIP_2 and PIP_3 are involved.

In contrast to its effect on Kir6.2-G334D/SUR1-KAKA channels, LY294002 caused a rapid reversible inhibition of Kir6.2-G334DΔC currents in nucleotide-free solution (52 ± 2%; n = 5), making it unsuitable for studying the role of PIP_2 on this channel.

Collectively, these experiments suggest that MgATP activation of K_{ATP} channels is largely mediated by Mg-nucleotide interaction with the NBDs of SUR1, but that there is a small (5–10%) component that is mediated by a different mechanism. We have not attempted to correct for this component, as it varies in magnitude and time course between patches, and is dependent on ATP concentration.

PKA is not involved in MgATP activation of Kir6.2-G334D currents

It has been proposed that MgATP enhances K_{ATP} channel activity via PKA-dependent phosphorylation (Ribalet et al., 1989; Béguin et al., 1999; Lin et al., 2000). The results described above argue that MgATP activation of Kir6.2-G334D is largely mediated via nucleotide interaction with the NBDs of SUR1. However, to conclusively exclude the possible involvement of PKA-dependent phosphorylation, we used the protein kinase A inhibitory peptide (PKIP) (Lin et al., 2000).

There was no significant difference in the extent of activation of Kir6.2-G334D/SUR1 currents in the presence of 1 mM MgATP (79 ± 9%; n = 6) and 1 mM MgATP plus 200 μg/ml PKIP (80 ± 9%; n = 6). We also examined the effect of PKIP on the small, slowly developing stimulatory effect of MgATP on Kir6.2ΔC-G334D currents. Again, the increase in current produced by 1 mM MgATP was not different in the absence (7.8 ± 0.9%; n = 6) or presence (7.2 ± 0.7%; n = 6) of 200 μg/ml PKIP.

Lin et al. (2000) have shown that the stimulatory effect of PKA on K_{ATP} channel activity is mediated by threonine 224 in the Kir6.2 subunit, and that the effect of PKA is abolished by mutation of T224 to alanine. As a further test for the possible involvement of PKA-dependent phosphorylation, we made the T224A mutation on the Kir6.2-G334D background and examined MgATP activation. We found that 1 mM MgATP activated Kir6.2-G334D-T224A/SUR1 channels to a similar extent as Kir6.2-G334D/SUR1 channels: 77 ± 9%

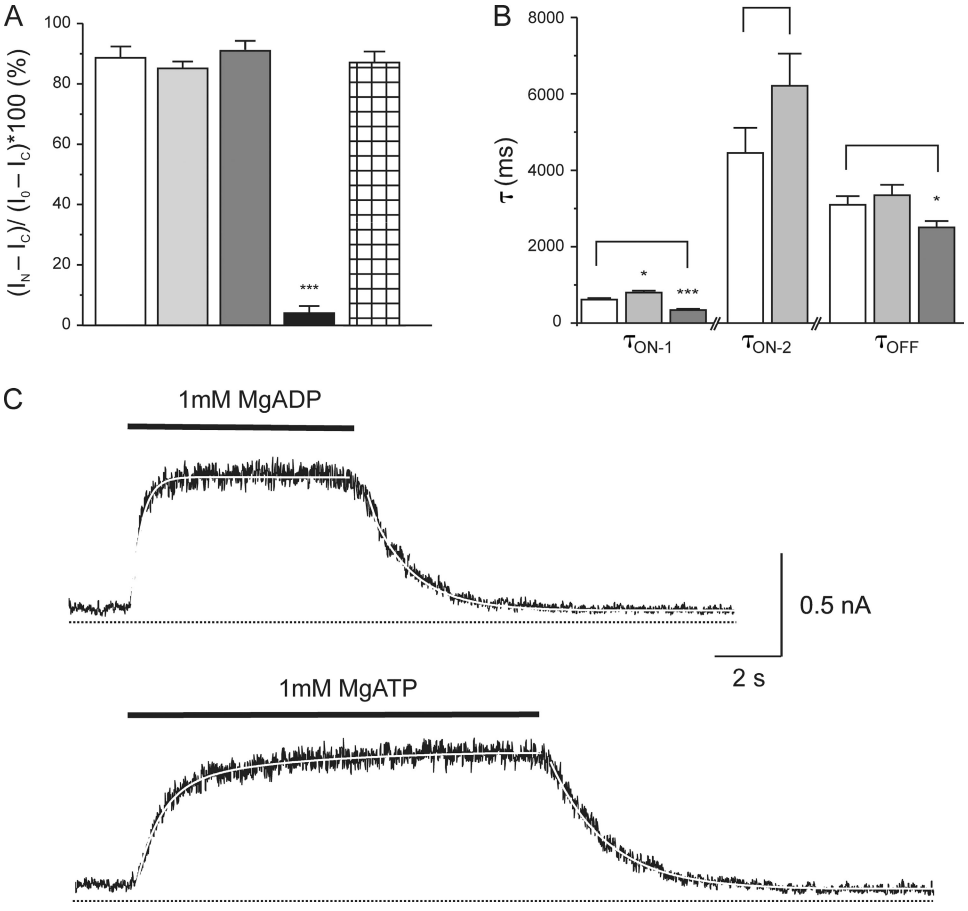

Figure 6. Effect of other Mg-nucleotides. (A) Mean increase in Kir6.2-G334D/SUR1 current in the presence of different nucleotides (refer to Materials and methods). White bar, 1 mM MgATP (n = 13); pale gray bar, 1 mM MgATPγS (n = 6); dark gray bar, 1 mM MgADP (n = 7); black bar, 1 mM MgAMP-PNP (n = 6); crosshatched bar, 1 mM MgAMP-PNP plus 1 mM MgATP (n = 6). ***, P < 0.001 (against MgATP). (B) Mean time constants (τ) of current activation (τ_{ON-1} and τ_{ON-2}) and deactivation (τ_{OFF}) by MgATP (white bars, n = 13), MgATPγS (pale gray bars, n = 6), and MgADP (dark gray bars, n = 7). *, P < 0.5; ***, P < 0.001 (against MgATP). (C) Time course of current activation and deactivation by 1 mM MgADP (top) and 1 mM MgATP (bottom). Nucleotide application is indicated by the bar, and the dotted line represents the zero current level. The white lines are the best fit of one (MgADP) or two (MgATP) exponential components for activation ($A_1 * e^{-t/\tau_1} + A_2 * e^{-t/\tau_2}$) and one for deactivation ($A * e^{-t/\tau}$). For MgADP: A_{ON-1} = 680 pA, τ_{ON-1} = 330 ms; A_{OFF} = 680 pA, τ_{OFF} = 1,320 ms. For MgATP: A_{ON-1} = 490 pA, τ_{ON-1} = 730 ms; A_{ON-2} = 180 pA, τ_{ON-2} = 4,060 ms; A_{OFF} = 670 pA; τ_{OFF} = 1,835 ms.

TABLE III

Single-channel parameters of Kir6.2-G334D/SUR1 channels in nucleotide-free solution and in the presence of 10 mM MgATP

Solution	P_O	τ_O	$\tau_{O,COR}$	τ_{B1}	a_{B1}	τ_{B2}	a_{B2}	τ_{B3}	A_{B3}	τ_B
		ms	*ms*	*ms*		*ms*		*ms*		*ms*
Control	0.34 ± 0.04	2.7 ± 0.3	1.8 ± 0.2	39 ± 4	0.57 ± 0.02	8.8 ± 2.4	0.28 ± 0.03	0.64 ± 0.18	0.15 ± 0.01	25 ± 2
10 mM MgATP	0.83 ± 0.01	3.0 ± 0.3	2.0 ± 0.2	256 ± 50	1	np	np	np	np	256 ± 50

P_O, single-channel open probability; τ_O, mean open time; $\tau_{O,COR}$, mean open time corrected for missed events (Proks et al., 2001); τ_{Bi} and a_{Bi}, burst durations and their corresponding amplitudes in the distribution of burst lengths (i = 1–3); τ_B, mean burst duration; np, not present in the distribution. Data are expressed as mean ± SEM (n = 3 each).

(n = 6) versus 79 ± 9% (n = 6). Finally, to investigate the possibility that K_{ATP} channel activity is modulated by endogenous PKA in intact cells (before patch excision), we measured P_O in cell-attached patches containing a low number of channels (one to five). There was no obvious difference in the mean P_O between Kir6.2-G334D-T224A/SUR1 channels (P_O = 0.76 ± 0.02; n = 6) and Kir6.2-G334D/SUR1 channels (P_O = 0.77 ± 0.01; n = 6).

Collectively, these experiments do not support the idea that activation by MgATP of either Kir6.2-G334D channels or Kir6.2ΔC-G334D channels involves PKA-dependent phosphorylation.

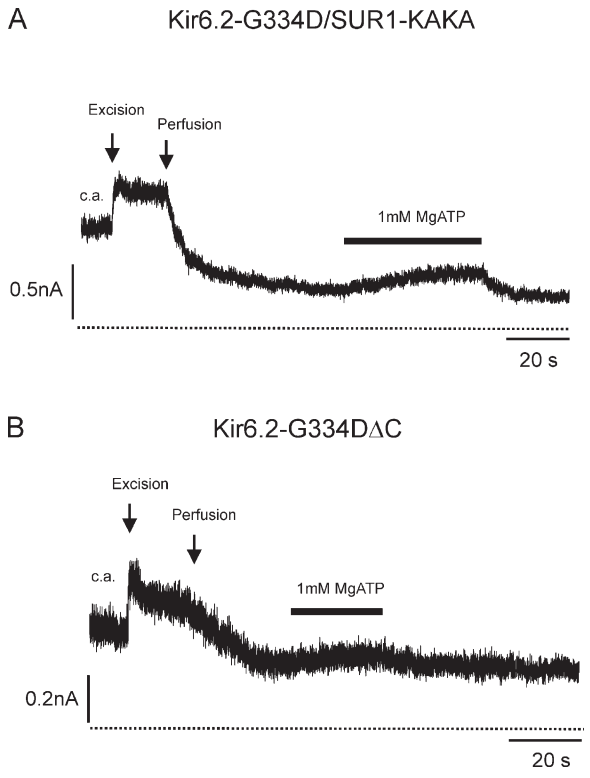

Figure 7. NBD-independent nucleotide activation. Representative examples of the effect of 1 mM MgATP on Kir6.2-G334D/SUR-KAKA channels (A) or Kir6.2-G334DΔC channels (B). Patch excision and the start of the perfusion with nucleotide-free solution are indicated by the arrows and MgATP application by the bars. The dotted line indicates the zero current level.

Effect of Mg-nucleotides on the single-channel kinetics

We next analyzed the effect of a maximal stimulatory concentration of 10 mM MgATP and 1 mM MgADP on the single-channel kinetics of Kir6.2-G334D/SUR1 channels (Figs. 8 and 9, and Tables III–VI). We selected only channels that showed stationary kinetics in nucleotide-free solution over a 10-min period. A similar increase in P_O was produced by MgATP and MgADP: from 0.46 ± 0.18 to 0.83 ± 0.01 (n = 3) for MgATP, and from 0.41 ± 0.16 to 0.83 ± 0.01 (n = 3) for MgADP. In both cases, the increase in P_O was caused by an increase in the mean open ($\tau_{O,COR}$) and mean burst (τ_B) duration, a decrease in the frequency (a_{C2} and a_{C3}) and mean duration (τ_{C2} and τ_{C3}) of the two shorter interburst components, and loss of the longest interburst component (a_{C4} = 0). In addition, both nucleotides eliminated the short burst components ($a_{B2} = a_{B3} = 0$) (Tables III and V). It is noteworthy that the properties of maximally activated channels are similar to those of mutant K_{ATP} channels with strongly impaired gating ($P_O(0)$ ~0.8; e.g., Trapp et al., 1998; Enkvetchakul et al., 2001; Proks et al., 2005a, 2007).

DISCUSSION

Our results show that MgATP and MgADP activate Kir6.2-G334D/SUR1 channels to similar extents, but that they do so with very different efficacies. The potency of MgADP (EC_{50}, 8 μM) was much greater than that of MgATP (EC_{50}, 112 μM), consistent with the idea that occupancy of the NBDs of SUR1 by MgADP drives channel opening, and that ATP must be hydrolyzed before it is effective. In agreement with this assumption, the EC_{50} for MgATP activation was similar to the K_i for MgATP displacement of 8-azido ATP binding to NBD2 of SUR1 (60 ± 26 μM) (Matsuo et al., 2000). Likewise, it is close to the K_m for MgATP hydrolysis obtained for purified SUR1 (0.1 mM) (de Wet et al., 2007), and not much lower than that found for the purified K_{ATP} channel complex (0.4 ± 0.2 mM) (Mikhailov et al., 2005).

The EC_{50} for MgADP activation (8 μM) is much smaller than the K_i for MgADP displacement of ATP binding to either NBD of SUR1, measured when SUR1 was expressed in the absence of Kir6.2 (26–100 μM) (Matsuo et al., 2000). The K_d for MgADP binding to the K_{ATP} channel complex has not been measured, but it clearly must be

TABLE IV

Single-channel parameters of Kir6.2-G334D/SUR1 channels in nucleotide-free solution and in the presence of 10 mM MgATP

Solution	τ_{C1}	a_{C1}	τ_{C2}	a_{C2}	τ_{C3}	a_{C3}	τ_{C4}	a_{C4}
	ms		*ms*		*ms*		*ms*	
Control	0.33 ± 0.01	0.904 ± 0.002	4.4 ± 1.2	0.042 ± 0.006	33 ± 7	0.042 ± 0.006	166 ± 30	0.012 ± 0.005
10 mM MgATP	0.34 ± 0.01	0.991 ± 0.002	2.9 ± 0.6	0.006 ± 0.002	16.7 ± 1.3	0.003 ± 0.001	np	np

τ_{Ci} and a_i, closed times and their corresponding amplitudes in the distribution of closed times (i = 1–4); np, not present in the distribution. Data are expressed as mean ± SEM (n = 3 each).

less than the EC_{50} for channel activation (i.e., <8 μM). Thus, our data suggest that that the affinity of SUR1 for MgADP may be modulated by the presence of Kir6.2, or that MgADP binding to SUR1 may be altered by the presence of MgATP. The latter idea is not unreasonable because MgADP binding to NBD2 has been shown to stabilize MgATP binding to NBD1 (Ueda et al., 1997), raising the possibility that nucleotide binding at the two NBDs interacts. Similarly, the affinity of Kir6.2 for ATP is enhanced by SUR1 (Tucker et al., 1997), indicating that interactions between the two subunits can influence nucleotide binding at the partner subunit.

Effects of other nucleotides

Our results demonstrate that the extent of activation by MgATP and MgATPγS (1 mM) was similar, indicating that

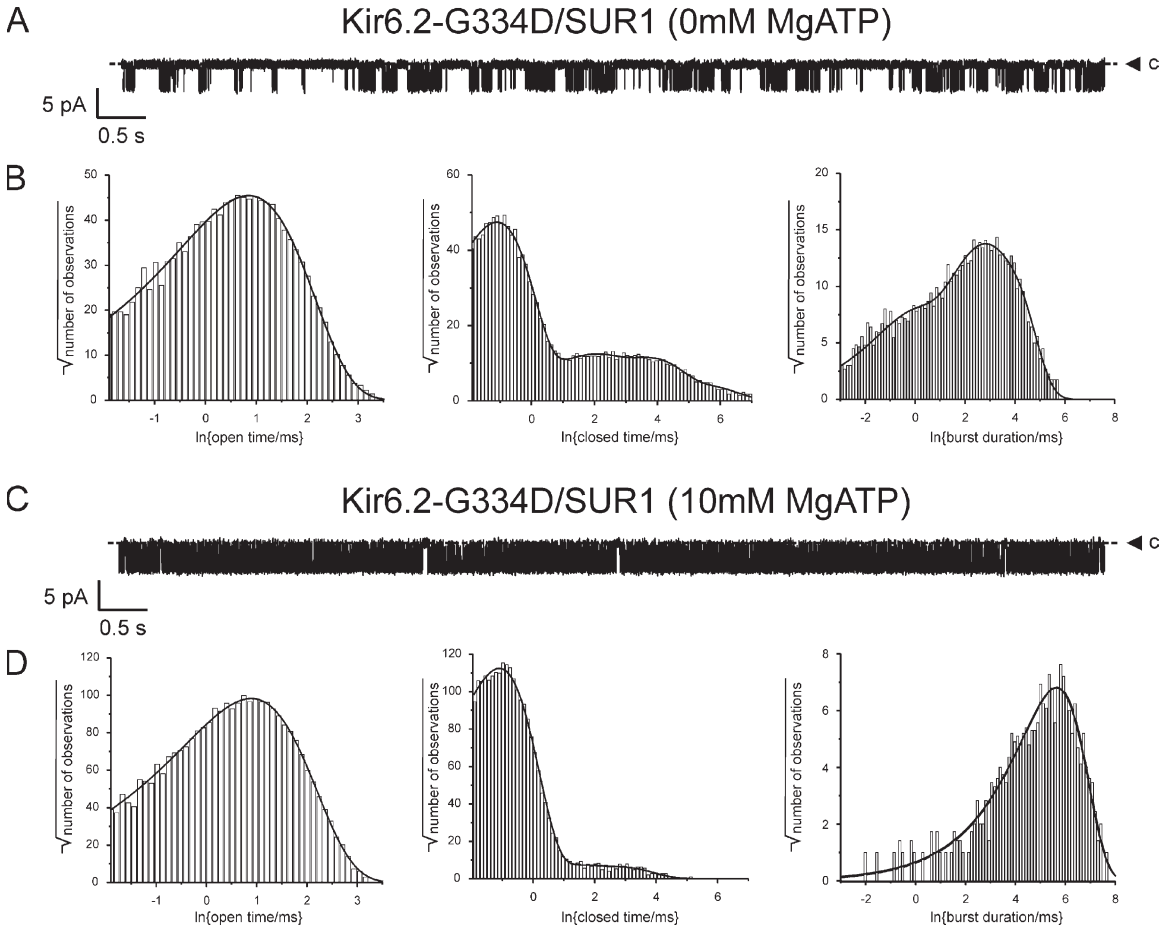

Figure 8. Effect of 10 mM MgATP on Kir6.2-G334D/SUR1 kinetics. (A and C) Single Kir6.2-G334D/SUR1 currents recorded at −60 mV from the same patch first in nucleotide-free solution (A), and then in the presence of 10 mM MgATP (C). c, the closed current level. (B and D) Distributions of open times (left), closed times (middle), and burst durations (right) in 0 mM MgATP (B; P_O = 0.26) and in 10 mM MgATP (D; P_O = 0.82). The distributions were fit with the following parameters. For 0 mM MgATP (B): open times: τ_O = 2.34 ms ($\tau_{O,COR}$ = 1.57 ms); closed times: τ_{C1} = 0.33 ms, a_{C1} = 0.901; τ_{C2} = 5.5 ms, a_{C2} = 0.043; τ_{C3} = 39 ms, a_{C3} = 0.049; τ_{C4} = 192 ms, a_{C4} = 0.007; burst times: τ_{B1} = 33 ms, a_{B1} = 0.53; τ_{B2} = 9.3 ms, a_{B2} = 0.34; τ_{B3} = 0.63 ms, a_{B3} = 0.13. The mean burst duration (τ_B) was 20.8 ms. For 10 mM MgATP (D): open times: τ_O = 2.73 ms ($\tau_{O,COR}$ = 1.75 ms); closed times: τ_{C1} = 0.33 ms, a_{C1} = 0.994; τ_{C2} = 2.5 ms, a_{C2} = 0.004; τ_{C3} = 14 ms, a_{C3} = 0.003; burst times: $\tau_B \equiv \tau_{B1}$ = 282 ms.

TABLE V

Single-channel parameters of Kir6.2-G334D/SUR1 channels in nucleotide-free solution and in the presence of 1 mM MgADP

Solution	P_O	τ_O (ms)	$\tau_{O,COR}$	τ_{B1}	a_{B1}	τ_{B2}	a_{B2}	τ_{B3}	a_{B2}	τ_B
		ms	*ms*	*ms*		*ms*		*ms*		*ms*
Control	0.36 ± 0.03	2.4 ± 0.7	1.6 ± 0.1	53 ± 15	0.66 ± 0.06	11 ± 6	0.23 ± 0.06	0.9 ± 0.5	0.11 ± 0.01	37 ± 9
1 mM MgADP	0.83 ± 0.01	2.7 ± 0.1	1.8 ± 0.1	246 ± 57	1	np	np	np	np	246 ± 57

P_O, single-channel open probability; τ_O, mean open time; $\tau_{O,COR}$, mean open time corrected for missed events (Proks et al., 2001); τ_{Bi} and a_{Bi}, burst durations and their corresponding amplitudes in the distribution of burst lengths (i = 1–3); τ_B, mean burst duration; np, not present in the distribution. Data are expressed as mean ± SEM (n = 3 each).

MgATPγS is hydrolyzed by SUR1. The fast time constant of activation by ATPγS was only slightly (30%) larger than that of MgATP, suggesting that any differences in the rate of hydrolysis are either small or that other steps in the activation process are rate-limiting.

In contrast, MgAMP-PNP had little or no stimulatory effect and was unable to prevent activation by MgATP. This suggests that MgAMP-PNP binds poorly to the NBDs of SUR1. Because AMP-PNP blocks wild-type channels (albeit not as effectively as ATP) (Schwanstecher et al., 1994), it may be useful as a tool when it is desired to block the channel at Kir6.2 without causing channel activation at SUR1.

On-rates and off-rates of activation

The time course of activation and deactivation were studied at near-saturating nucleotide-binding concentrations. The off-rate must represent the sum of nucleotide unbinding and the rate of channel closure. The latter can be expected to be independent of nucleotide. Because it is believed that channel activation is produced by the MgADP-bound state, one might expect the off-rate would be similar for both MgADP and MgATP. There are three possible explanations for the fact that this is not the case: (1) some channels are in the MgATP-bound state when nucleotide is removed and must undergo MgATP hydrolysis before they close; (2) some channels are in the MgATP-bound state when nucleotide is removed and undergo MgATP unbinding, which occurs more slowly than that of MgADP; and (3) if both the MgADP and the MgADP.Pi states of the hydrolytic cycle support channel activation, this might explain the slower off-rate of MgATP compared with MgADP.

The time constant of channel activation by MgADP was much smaller than that of deactivation. This might be attributable to a faster rate of MgADP binding than unbinding: a similar conclusion was reached for cardiac K_{ATP} channels (Bienengraeber et al., 2004). Alternatively, the rate of channel opening might be faster than that of channel closing. This could happen if the binding of MgADP to a single SUR1 subunit is needed to open the channel but additional molecules subsequently bind and MgADP must unbind from all subunits before the channel can close.

The on-rate for MgATP activation must include the additional time required for nucleotide hydrolysis. This may explain why activation is faster for MgADP than for MgATP. The very similar rates of activation and deactivation for MgATP and MgATPγS indicate that there is little difference in any of the reaction cycle rates for these nucleotides.

Properties of NBD-independent activation

Consistent with previous results (Gribble et al., 1997b, 1998; Shyng et al., 1997), channel activation by Mg-nucleotides requires functionally intact NBDs. A small increase in current in response to MgATP is observed when the Walker A lysines are mutated, or for Kir6.2-G334DΔC alone. The simplest explanation is that this represents current activation by PIP_2 generated by endogenous kinases when MgATP is present. However, the lack of effect of a PIP_2 antibody makes this less likely. Whatever the mechanism, these results serve to show that all of the activation produced by MgADP, and ∼90% of that produced by MgATP, is mediated via the NBDs of SUR1.

Single-channel analysis

At saturating binding concentrations, ATP and ADP appear to have virtually identical effects on the single-channel kinetics of Kir6.2-G334D/SUR1 channels. Thus, prehydrolytic states appear to have no influence on the

TABLE VI

Single-channel parameters of Kir6.2-G334D/SUR1 channels in nucleotide-free solution and in the presence of 1 mM MgADP

Solution	τ_{C1}	a_{C1}	τ_{C2}	a_{C2}	τ_{C3}	a_{C3}	τ_{C4}	a_{C4}
	ms		ms		ms		ms	
Control	0.34 ± 0.01	0.934 ± 0.011	7.4 ± 1.8	0.022 ± 0.008	38 ± 8	0.035 ± 0.006	306 ± 132	0.008 ± 0.005
1 mM MgADP	0.36 ± 0.01	0.988 ± 0.002	4.0 ± 1.0	0.005 ± 0.002	16.8 ± 2.6	0.007 ± 0.001	np	np

τ_{Ci} and a_i, closed times and their corresponding amplitudes in the distribution of closed times (i = 1–4); np, not present in the distribution. Data are expressed as mean ± SEM (n = 3 each).

gating of K_{ATP} channels, at least when Mg-nucleotide inhibition at Kir6.2 is abolished by the G334D mutation. It remains possible, however, that these states may affect the gating of K_{ATP} channels when ATP is bound to Kir6.2.

As previously shown for the effects of MgATP on Kir6.2/SUR1 (Li et al., 2002) and MgUDP on Kir6.2/SUR2A channels (Alekseev et al., 1998), adenosine nucleotides affect both the open and the interburst states of the channel, producing an increase in the duration of openings and bursts, and a decrease in the frequency and duration of interburst closures. The lack of an effect of MgADP on the brief intraburst closings indicates that the nucleotide has little or no effect on the "fast" gate that governs the intraburst closures, as is also the case for the inhibitory effect of ATP at Kir6.2 (Li et al., 2002). Rather, MgADP operates upon the "slow" gate that governs the long interburst closures. The results further indicate that even under conditions of maximal activation, the slow gate can still close.

Implications for modulation of Kir6.2/SUR1 channel activity by Mg-nucleotides in excised patches

Can we now predict the behavior of the wild-type channel in the presence of Mg-nucleotides? Fig. 10 A shows the concentration-inhibition curve for ADP for wild-type channels, measured in the absence of added Mg^{2+} to exclude any interaction with SUR1, and the MgADP concentration–activation curve measured for Kir6.2-G334D/SUR1 channels to exclude any interaction with Kir6.2. The third curve shows the concentration–response relation for wild-type channels in MgADP, where both activation and inhibition are present. This exhibits a bell-shaped dependence on MgADP concentration with a peak at ~50 μM MgADP, in agreement with a previous report (Hopkins et al., 1992). It is evident that the increase in the wild-type K_{ATP} current at low MgADP concentrations (<40 μM) is paralleled by a similar increase in Kir6.2-G334D/SUR1 current, and that the peak current

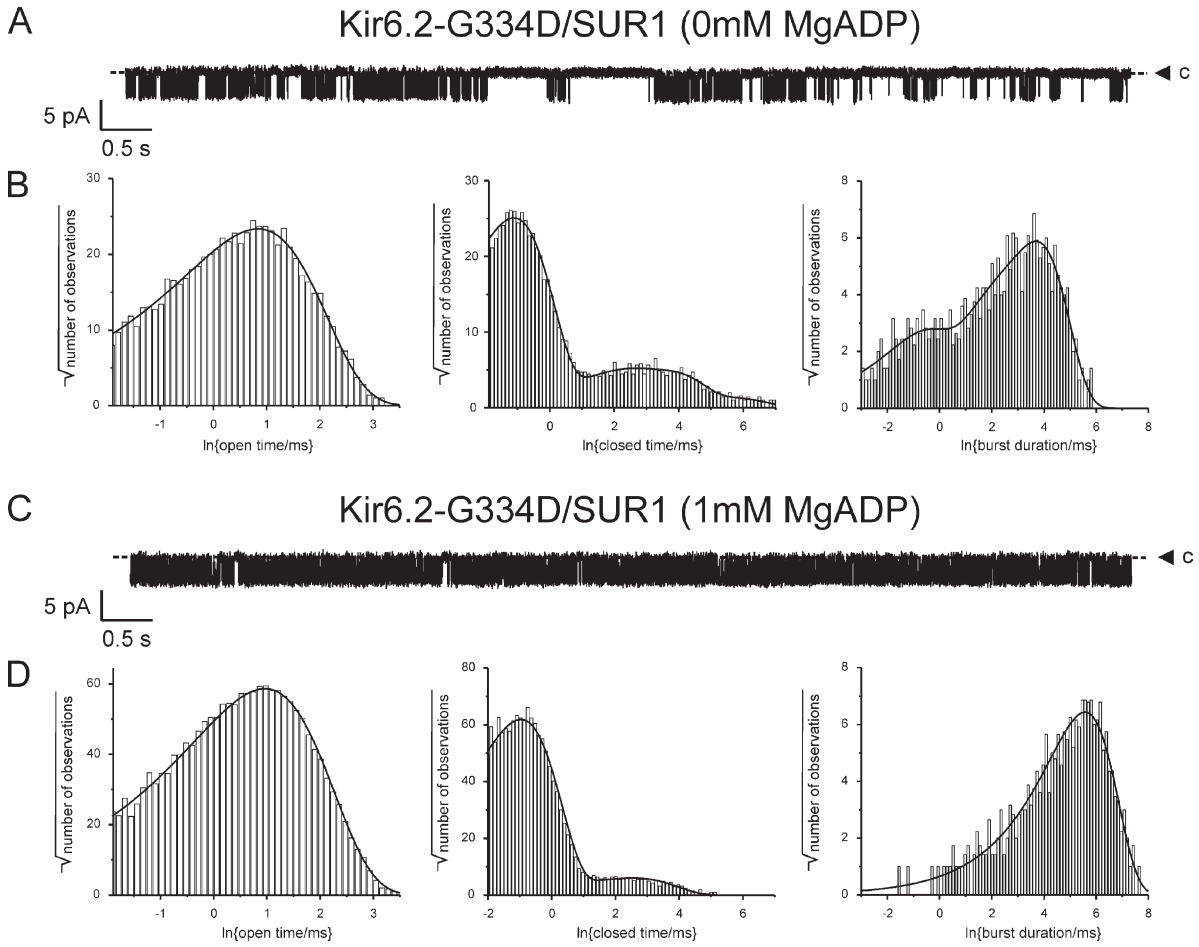

Figure 9. Effect of 1 mM MgADP on Kir6.2-G334D/SUR1 kinetics. (A and C) Single Kir6.2-G334D/SUR1 currents recorded at −60 mV from the same patch first in nucleotide-free solution (A), and then in 1 mM MgADP (C). (B and D) Distributions of open times (left), closed times (middle), and burst durations (right) in 0 mM MgADP (B; $P_O = 0.39$) and 1 mM MgADP (D; $P_O = 0.82$). The distributions were fit with the following parameters. For 0 mM MgADP (B): open times: $\tau_O = 2.31$ ms ($\tau_{O,COR} = 1.51$ ms); closed times: $\tau_{C1} = 0.33$ ms, $a_{C1} = 0.942$; $\tau_{C2} = 7.3$ ms, $a_{C2} = 0.021$; $\tau_{C3} = 36$ ms, $a_{C3} = 0.034$; $\tau_{C4} = 230$ ms, $a_{C4} = 0.003$; burst times: $\tau_{B1} = 41$ ms, $a_{B1} = 0.770$; $\tau_{B2} = 5.6$ ms, $a_{B2} = 0.115$; $\tau_{B3} = 0.46$ ms, $a_{B3} = 0.115$. The mean burst duration (τ) was 32.3 ms. For 1 mM MgADP (D): open times: $\tau_O = 2.61$ ms ($\tau_{O,COR} = 1.77$ ms); closed times: $\tau_{C1} = 0.38$ ms, $a_{C1} = 0.990$; $\tau_{C2} = 3.8$ ms, $a_{C2} = 0.001$; $\tau_{C3} = 14$ ms, $a_{C3} = 0.009$; burst times: $\tau_B \equiv \tau_{B1} = 263$ ms.

is close to the IC_{50} for ADP inhibition in Mg-free solution (62 μM, this paper; 64 μM, Dabrowski et al., 2003).

It has been previously argued that the stimulatory effect of MgADP is mediated by a reduction in MgATP binding to Kir6.2 (Nichols et al., 1996; Shyng et al., 1997; Matsuo et al., 2000; John et al., 2001; Abraham et al., 2002). The fact that MgADP is able to stimulate channel activity in the complete absence of MgATP indicates that this cannot be the only mechanism of channel activation, and that MgADP (and MgATP) must have a direct effect on channel gating. Nevertheless, it remains possible that Mg-nucleotide interaction with SUR1 may also impair nucleotide binding to Kir6.2.

If we assume that the activatory and inhibitory effects of MgADP are independent, then the concentration–response curve for wild-type channels exposed to MgADP may be described by the product of two Hill equations (Eq. 3). When we used the EC_{50} determined for MgADP activation of Kir6.2-G334D/SUR1 (8 μM) and the IC_{50} measured for ADP inhibition of Kir6.2/SUR1 channels

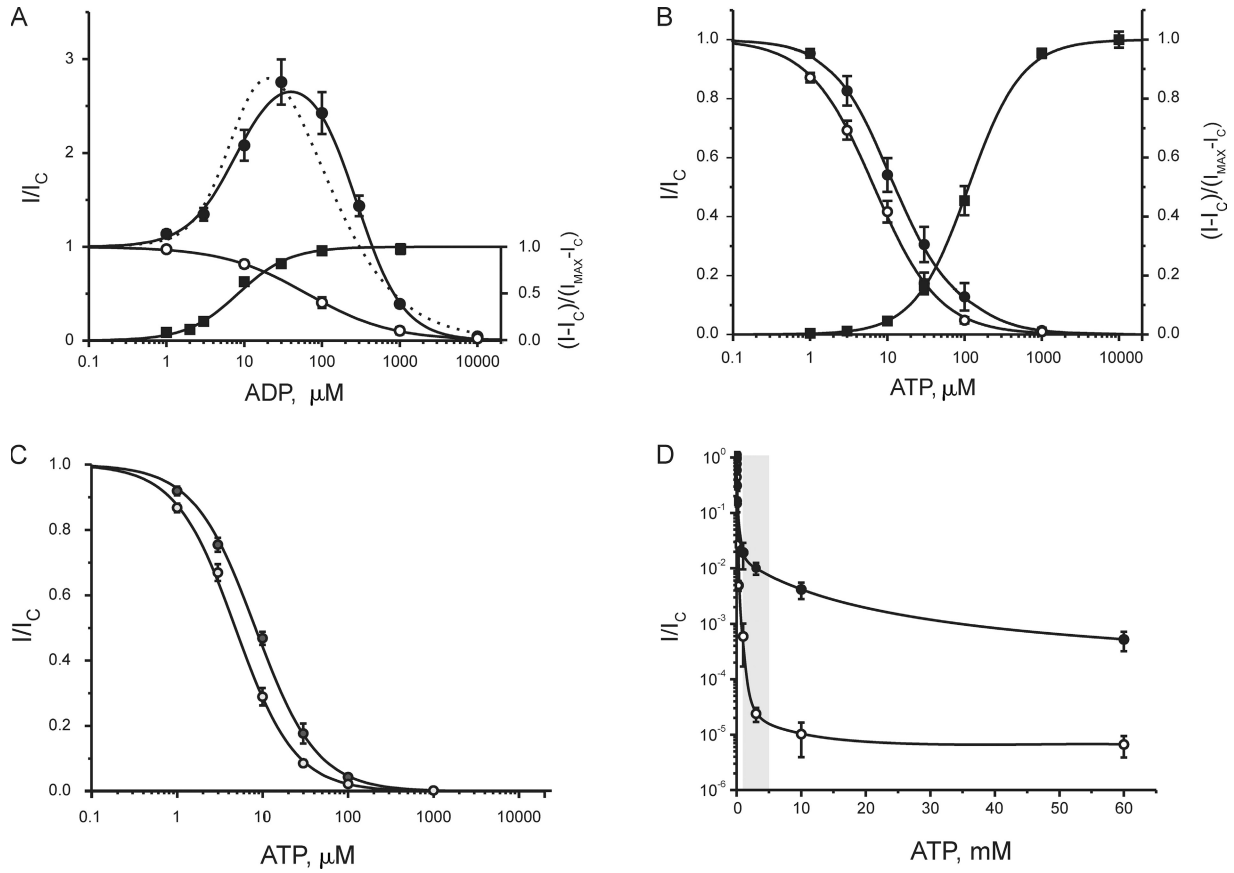

Figure 10. Comparison of the activatory and inhibitory effects of Mg-nucleotides. (A) Concentration–response relationships for activation and inhibition of macroscopic K_{ATP} currents by ADP. Inhibition was measured for Kir6.2/SUR1 currents in the absence of Mg^{2+} (open circles; $n = 6$). Activation was measured for Kir6.2-G334D/SUR1 currents in the presence of Mg^{2+} (filled squares; $n = 8$; data from Fig. 5 C). Filled circles ($n = 15$) indicate data obtained for Kir6.2/SUR1 currents in the presence of Mg^{2+}, where activation and inhibition are simultaneously present. The solid lines are the best fit of Eqs. 1–3 to the mean data. For Kir6.2-G334D/SUR1 channels, data were fit with Eq. 1, $EC_{50} = 7.7$ μM and $h = 1.30$. For Kir6.2/SUR1 channels, data in Mg-free solution were fit with Eq. 2, $IC_{50} = 62$ μM and $h = 0.81$, and data in Mg-containing solution were fit with Eq. 3 using fixed activation parameters ($EC_{50} = 8$ μM and $h_2 = 1.3$) and $a = 2$; $IC_{50} = 280$ μM and $h_1 = 1.4$ for inhibition. The dotted line is best fit of the data for Kir6.2/SUR1 in Mg-containing solution assuming no interaction between the activatory and inhibitory sites (IC_{50} was fixed at 62 μM and EC_{50} at 8 μM) and $a = 2.5$, $h_1 = 1.3$, and $h_2 = 1.3$. (B) Concentration–response relationships for activation and inhibition of macroscopic K_{ATP} currents by ATP. Inhibition was measured for Kir6.2/SUR1 currents in the absence of Mg^{2+} (open circles; $n = 6$). Activation was measured for Kir6.2-G334D/SUR1 currents in the presence of Mg^{2+} (filled squares; $n = 8$; data from Fig. 5 C). Filled circles ($n = 8$) indicate data obtained for Kir6.2/SUR1 currents in the presence of Mg^{2+}, where activation and inhibition are simultaneously present. For Kir6.2-G334D/SUR1 channels, the line through the mean data were fit with Eq. 1, $EC_{50} = 112$ μM and $h = 1.25$. For Kir6.2/SUR1 channels in the absence of Mg^{2+}, the line through the mean data are the best fit of Eq. 2, with $IC_{50} = 7.1$ μM and $h = 1.1$. For Kir6.2/SUR1 channels, data in Mg-containing solution were fit with Eq. 2, with $IC_{50} = 14$ μM and $h = 1.0$. (C) Concentration–inhibition relationships for Kir6.2/SUR1-KAKA currents in the absence (open circles; $n = 8$) and presence of Mg^{2+} (gray circles; $n = 8$). The lines through the mean data are the best fit of Eq. 2, with $IC_{50} = 4.8$ μM and $h = 1.2$ for Mg^{2+}-free solution, and $IC_{50} = 8.3$ μM and $h = 1.2$ for Mg^{2+} solution. (D) Concentration–response inhibition relationships for Kir6.2/SUR1 currents in the absence (open circles; $n = 8$) or presence of Mg^{2+} (filled circles; $n = 8$). The physiological range of $[ATP]_i$ is shown by the bar. The lines are drawn by eye.

in the absence of Mg^{2+} (62 µM), we obtained a rather poor fit to the data for wild-type channels in the presence of Mg^{2+} (Fig. 10 A, dotted line). A much better fit was obtained if we assumed that MgADP activation impairs ADP binding to Kir6.2, and allowed IC_{50} to be a free parameter. In this case, the relationship between MgADP and the wild-type K_{ATP} current was well fit with the product of two Hill equations and an IC_{50} of 280 µM for ADP block (Fig. 10 A, solid line). This value is ∼4.5-fold greater than that measured in Mg-free solution, and it is consistent with nucleotide interactions at SUR1 reducing the affinity of Kir6.2 for ADP. However, further studies are required to substantiate this idea and to determine the underlying mechanism.

In contrast to MgADP, comparison of the MgATP response curve for wild-type channels with those for ATP inhibition and MgATP activation (Fig. 10 B) reveals a puzzling discrepancy at low ATP concentrations (≤10 µM). Namely, the inhibitory effect of MgATP is shifted to higher ATP concentrations with respect to that in the absence of Mg^{2+}, yet there is no substantial activatory effect of MgATP at these concentrations (at least as measured for Kir6.2-G334D/SUR1 channels). There are several possible explanations for this effect. First, the G334D mutation may somehow impair binding of MgATP (but not MgADP) to the NBDs of SUR1. Second, ATP binding to wild-type Kir6.2 may enhance the affinity of the NBDs for Mg-nucleotide. Third, this effect may involve an unknown mechanism with a high affinity for MgATP.

The two first hypotheses assume that the shift in the ATP dose–response curve in the presence of Mg^{2+} at [ATP] ≤10 µM is mediated by nucleotide interaction with the NBDs. If this is the case, no shift should occur when the NBDs are not operational, as when the W_A lysines are mutated. However, as shown in Fig. 10 C, Kir6.2/SUR1-KAKA channels exhibited a similar shift in ATP sensitivity when Mg^{2+} is present to that of the wild-type channel. This result suggests that the Mg^{2+}-induced shift in the ATP dose–response relation, as least at low ATP concentrations, is produced via a mechanism that is independent of the NBDs but requires Mg^{2+}. This cannot be a PKA-dependent phosphorylation because we found no difference in the effect of 10 µM MgATP on Kir6.2/SUR1 currents in the presence of 200 µg/ml PKIP (the fractional current remaining in the presence of the nucleotide was 0.58 ± 0.07, $n = 6$, in both the presence and absence of the inhibitor).

Collectively, these results indicate that NBD-dependent activation contributes little to the increase in the value of IC_{50} for channel inhibition by ATP found in the presence of Mg^{2+} (from 7 to 12 µM; Fig. 10 B). Instead, it is expected to alter the magnitude of the ATP-resistant current at higher ATP concentrations and to account for the small ATP-resistant current seen at $[ATP]_i$ >1 mM.

As shown in Fig. 10 B, Mg^{2+} has little apparent effect on the K_{ATP} channel sensitivity to ATP inhibition at [ATP] >1 mM when plotted on linear scale. However, if we display the current amplitude on log scale, it becomes obvious that there is actually a very marked (>100-fold) difference in the current at high [ATP] (1–60 mM) in the presence and absence of Mg^{2+} (Fig. 10 D). This difference persists over the physiological range of nucleotide concentrations found in pancreatic β cells (1–5 mM; denoted by the bar in Fig. 10 D). Because the resting membrane potential of the β cell is very sensitive to small changes in the K_{ATP} current (Tarasov et al., 2006; Proks and Ashcroft, 2009), the ATP-resistant current produced by NBD-mediated activation is expected to exert a strong influence on β cell electrical excitability.

This work was supported by grants from the European Union (BioSim LHSB-CT-2004-005137, EuroDia SHM-CT-2006-518513, and EDICT HEALTH-F4-2007-201924) and the Wellcome Trust.

Lawrence G. Palmer served as editor.

Submitted: 12 May 2010
Accepted: 3 September 2010

REFERENCES

Abraham, M.R., V.A. Selivanov, D.M. Hodgson, D. Pucar, L.V. Zingman, B. Wieringa, P.P. Dzeja, A.E. Alekseev, and A. Terzic. 2002. Coupling of cell energetics with membrane metabolic sensing. Integrative signaling through creatine kinase phosphotransfer disrupted by M-CK gene knock-out. *J. Biol. Chem.* 277:24427–24434. doi:10.1074/jbc.M201777200

Aittoniemi, J., C. Fotinou, T.J. Craig, H. de Wet, P. Proks, and F.M. Ashcroft. 2009. Review. SUR1: a unique ATP-binding cassette protein that functions as an ion channel regulator. *Philos. Trans. R. Soc. Lond. B Biol. Sci.* 364:257–267. doi:10.1098/rstb.2008.0142

Alekseev, A.E., P.A. Brady, and A. Terzic. 1998. Ligand-insensitive state of cardiac ATP-sensitive K^+ channels. Basis for channel opening. *J. Gen. Physiol.* 111:381–394. doi:10.1085/jgp.111.2.381

Antcliff, J.F., S. Haider, P. Proks, M.S.P. Sansom, and F.M. Ashcroft. 2005. Functional analysis of a structural model of the ATP-binding site of the K_{ATP} channel Kir6.2 subunit. *EMBO J.* 24:229–239. doi:10.1038/sj.emboj.7600487

Ashcroft, F.M. 2007. The Walter B. Cannon Physiology in Perspective Lecture, 2007. ATP-sensitive K^+ channels and disease: from molecule to malady. *Am. J. Physiol. Endocrinol. Metab.* 293:E880–E889. doi:10.1152/ajpendo.00348.2007

Baukrowitz, T., U. Schulte, D. Oliver, S. Herlitze, T. Krauter, S.J. Tucker, J.P. Ruppersberg, and B. Fakler. 1998. PIP_2 and PIP as determinants for ATP inhibition of K_{ATP} channels. *Science.* 282:1141–1144. doi:10.1126/science.282.5391.1141

Béguin, P., K. Nagashima, M. Nishimura, T. Gonoi, and S. Seino. 1999. PKA-mediated phosphorylation of the human K_{ATP} channel: separate roles of Kir6.2 and SUR1 subunit phosphorylation. *EMBO J.* 18:4722–4732. doi:10.1093/emboj/18.17.4722

Bienengraeber, M., T.M. Olson, V.A. Selivanov, E.C. Kathmann, F. O'Cochlain, F. Gao, A.B. Karger, J.D. Ballew, D.M. Hodgson, L.V. Zingman, et al. 2004. ABCC9 mutations identified in human dilated cardiomyopathy disrupt catalytic KATP channel gating. *Nat. Genet.* 36:382–387.

Bokvist, K., C. Ammälä, F.M. Ashcroft, P.O. Berggren, O. Larsson, and P. Rorsman. 1991. Separate processes mediate nucleotide-induced inhibition and stimulation of the ATP-regulated K^+-channels in mouse pancreatic β-cells. *Proc Biol Sci.* 243:139–144. doi:10.1098/rspb.1991.0022

Clement, J.P., IV, K. Kunjilwar, G. Gonzalez, M. Schwanstecher, U. Panten, L. Aguilar-Bryan, and J. Bryan. 1997. Association and stoichiometry of K_{ATP} channel subunits. *Neuron.* 18:827–838. doi:10.1016/S0896-6273(00)80321-9

Dabrowski, M., S. Trapp, and F.M. Ashcroft. 2003. Pyridine nucleotide regulation of the K_{ATP} channel Kir6.2/SUR1 expressed in *Xenopus* oocytes. *J. Physiol.* 550:357–363. doi:10.1113/jphysiol.2003.041715

Davies, N.W., N.B. Standen, and P.R. Stanfield. 1992. The effect of intracellular pH on ATP-dependent potassium channels of frog skeletal muscle. *J. Physiol.* 445:549–568.

de Wet, H., M.V. Mikhailov, C. Fotinou, M. Dreger, T.J. Craig, C. Vénien-Bryan, and F.M. Ashcroft. 2007. Studies of the ATPase activity of the ABC protein SUR1. *FEBS J.* 274:3532–3544. doi:10.1111/j.1742-4658.2007.05879.x

Drain, P., L.H. Li, and J. Wang. 1998. K_{ATP} channel inhibition by ATP requires distinct functional domains of the cytoplasmic C terminus of the pore-forming subunit. *Proc. Natl. Acad. Sci. USA.* 95:13953–13958. doi:10.1073/pnas.95.23.13953

Enkvetchakul, D., G. Loussouarn, E. Makhina, and C.G. Nichols. 2001. ATP interaction with the open state of the K_{ATP} channel. *Biophys. J.* 80:719–728. doi:10.1016/S0006-3495(01)76051-1

Fan, Z., and J.C. Makielski. 1997. Anionic phospholipids activate ATP-sensitive potassium channels. *J. Biol. Chem.* 272:5388–5395. doi:10.1074/jbc.272.9.5388

Findlay, I., and M.J. Dunne. 1986. ATP maintains ATP-inhibited K^+ channels in an operational state. *Pflugers Arch.* 407:238–240. doi:10.1007/BF00580683

Furukawa, T., L. Virág, T. Sawanobori, and M. Hiraoka. 1993. Stilbene disulfonates block ATP-sensitive K^+ channels in guinea pig ventricular myocytes. *J. Membr. Biol.* 136:289–302.

Gillis, K.D., W.M. Gee, A. Hammoud, M.L. McDaniel, L.C. Falke, and S. Misler. 1989. Effects of sulfonamides on a metabolite-regulated ATP_i-sensitive K^+ channel in rat pancreatic β-cells. *Am. J. Physiol.* 257:C1119–C1127.

Gribble, F.M., R. Ashfield, C. Ammälä, and F.M. Ashcroft. 1997a. Properties of cloned ATP-sensitive K^+ currents expressed in *Xenopus* oocytes. *J. Physiol.* 498:87–98.

Gribble, F.M., S.J. Tucker, and F.M. Ashcroft. 1997b. The essential role of the Walker A motifs of SUR1 in K_{ATP} channel activation by Mg-ADP and diazoxide. *EMBO J.* 16:1145–1152. doi:10.1093/emboj/16.6.1145

Gribble, F.M., S.J. Tucker, T. Haug, and F.M. Ashcroft. 1998. MgATP activates the β cell K_{ATP} channel by interaction with its SUR1 subunit. *Proc. Natl. Acad. Sci. USA.* 95:7185–7190. doi:10.1073/pnas.95.12.7185

Hopkins, W.F., S. Fatherazi, B. Peter-Riesch, B.E. Corkey, and D.L. Cook. 1992. Two sites for adenine-nucleotide regulation of ATP-sensitive potassium channels in mouse pancreatic β-cells and HIT cells. *J. Membr. Biol.* 129:287–295.

John, S.A., J.N. Weiss, and B. Ribalet. 2001. Regulation of cloned ATP-sensitive K channels by adenine nucleotides and sulfonylureas: interactions between SUR1 and positively charged domains on Kir6.2. *J. Gen. Physiol.* 118:391–405. doi:10.1085/jgp.118.4.391

Li, L., X. Geng, and P. Drain. 2002. Open state destabilization by ATP occupancy is mechanism speeding burst exit underlying K_{ATP} channel inhibition by ATP. *J. Gen. Physiol.* 119:105–116. doi:10.1085/jgp.119.1.105

Lin, Y.F., Y.N. Jan, and L.Y. Jan. 2000. Regulation of ATP-sensitive potassium channel function by protein kinase A-mediated phosphorylation in transfected HEK293 cells. *EMBO J.* 19:942–955. doi:10.1093/emboj/19.5.942

Magleby, K.L., and B.S. Pallotta. 1983. Burst kinetics of single calcium-activated potassium channels in cultured rat muscle. *J. Physiol.* 344:605–623.

Markworth, E., C. Schwanstecher, and M. Schwanstecher. 2000. ATP^{4-} mediates closure of pancreatic beta-cell ATP-sensitive potassium channels by interaction with 1 of 4 identical sites. *Diabetes.* 49:1413–1418. doi:10.2337/diabetes.49.9.1413

Masia, R., J.C. Koster, S. Tumini, F. Chiarelli, C. Colombo, C.G. Nichols, and F. Barbetti. 2007. An ATP-binding mutation (G334D) in KCNJ11 is associated with a sulfonylurea-insensitive form of developmental delay, epilepsy, and neonatal diabetes. *Diabetes.* 56:328–336. doi:10.2337/db06-1275

Matsuo, M., K. Tanabe, N. Kioka, T. Amachi, and K. Ueda. 2000. Different binding properties and affinities for ATP and ADP among sulfonylurea receptor subtypes, SUR1, SUR2A, and SUR2B. *J. Biol. Chem.* 275:28757–28763. doi:10.1074/jbc.M004818200

Mikhailov, M.V., J.D. Campbell, H. de Wet, K. Shimomura, B. Zadek, R.F. Collins, M.S. Sansom, R.C. Ford, and F.M. Ashcroft. 2005. 3-D structural and functional characterization of the purified K_{ATP} channel complex Kir6.2-SUR1. *EMBO J.* 24:4166–4175. doi:10.1038/sj.emboj.7600877

Miki, T., and S. Seino. 2005. Roles of K_{ATP} channels as metabolic sensors in acute metabolic changes. *J. Mol. Cell. Cardiol.* 38:917–925. doi:10.1016/j.yjmcc.2004.11.019

Nichols, C.G., S.L. Shyng, A. Nestorowicz, B. Glaser, J.P. Clement IV, G. Gonzalez, L. Aguilar-Bryan, M.A. Permutt, and J. Bryan. 1996. Adenosine diphosphate as an intracellular regulator of insulin secretion. *Science.* 272:1785–1787. doi:10.1126/science.272.5269.1785

Proks, P., and F.M. Ashcroft. 1993. Modification of K_{ATP} channels in pancreatic β-cells by trypsin. *Pflugers Arch.* 424:63–72. doi:10.1007/BF00375103

Proks, P., and F.M. Ashcroft. 2009. Modeling K_{ATP} channel gating and its regulation. *Prog. Biophys. Mol. Biol.* 99:7–19. doi:10.1016/j.pbiomolbio.2008.10.002

Proks, P., C.E. Capener, P. Jones, and F.M. Ashcroft. 2001. Mutations within the P-loop of Kir6.2 modulate the intraburst kinetics of the ATP-sensitive potassium channel. *J. Gen. Physiol.* 118:341–353. doi:10.1085/jgp.118.4.341

Proks, P., C. Girard, S. Haider, A.L. Gloyn, A.T. Hattersley, M.S.P. Sansom, and F.M. Ashcroft. 2005a. A gating mutation at the internal mouth of the Kir6.2 pore is associated with DEND syndrome. *EMBO Rep.* 6:470–475. doi:10.1038/sj.embor.7400393

Proks, P., C. Girard, and F.M. Ashcroft. 2005b. Functional effects of KCNJ11 mutations causing neonatal diabetes: enhanced activation by MgATP. *Hum. Mol. Genet.* 14:2717–2726. doi:10.1093/hmg/ddi305

Proks, P., K. Shimomura, T.J. Craig, C.A. Girard, and F.M. Ashcroft. 2007. Mechanism of action of a sulphonylurea receptor SUR1 mutation (F132L) that causes DEND syndrome. *Hum. Mol. Genet.* 16:2011–2019. doi:10.1093/hmg/ddm149

Qin, D.Y., M. Takano, and A. Noma. 1989. Kinetics of ATP-sensitive K^+ channel revealed with oil-gate concentration jump method. *Am. J. Physiol.* 257:H1624–H1633.

Ribalet, B., S. Ciani, and G.T. Eddlestone. 1989. ATP mediates both activation and inhibition of K_{ATP} channel activity via cAMP-dependent protein kinase in insulin-secreting cell lines. *J. Gen. Physiol.* 94:693–717. doi:10.1085/jgp.94.4.693

Rosado, J.A., and S.O. Sage. 2000. A role for the actin cytoskeleton in the initiation and maintenance of store-mediated calcium entry in human platelets. *Trends Cardiovasc. Med.* 10:327–332. doi:10.1016/S1050-1738(01)00073-1

Schwanstecher, C., C. Dickel, and U. Panten. 1994. Interaction of tolbutamide and cytosolic nucleotides in controlling the ATP-sensitive K^+ channel in mouse beta-cells. *Br. J. Pharmacol.* 111:302–310.

Shyng, S.L., and C.G. Nichols. 1998. Membrane phospholipid control of nucleotide sensitivity of K_{ATP} channels. *Science.* 282:1138–1141. doi:10.1126/science.282.5391.1138

Shyng, S.L., T. Ferrigni, and C.G. Nichols. 1997. Regulation of K_{ATP} channel activity by diazoxide and MgADP. Distinct functions of the two nucleotide binding folds of the sulfonylurea receptor. *J. Gen. Physiol.* 110:643–654. doi:10.1085/jgp.110.6.643

Silberberg, S.D., and K.L. Magleby. 1993. Preventing errors when estimating single channel properties from the analysis of current fluctuations. *Biophys. J.* 65:1570–1584. doi:10.1016/S0006-3495(93)81196-2

Tarasov, A.I., H.J. Welters, S. Senkel, G.U. Ryffel, A.T. Hattersley, N.G. Morgan, and F.M. Ashcroft. 2006. A Kir6.2 mutation causing neonatal diabetes impairs electrical activity and insulin secretion from INS-1 beta-cells. *Diabetes.* 55:3075–3082. doi:10.2337/db06-0637

Trapp, S., P. Proks, S.J. Tucker, and F.M. Ashcroft. 1998. Molecular analysis of K_{ATP} channel gating and implications for channel inhibition by ATP. *J. Gen. Physiol.* 112:333–349.

Tucker, S.J., F.M. Gribble, C. Zhao, S. Trapp, and F.M. Ashcroft. 1997. Truncation of Kir6.2 produces ATP-sensitive K^+ channels in the absence of the sulphonylurea receptor. *Nature.* 387:179–183. doi:10.1038/387179a0

Ueda, K., N. Inagaki, and S. Seino. 1997. MgADP antagonism to Mg^{2+}-independent ATP binding of the sulfonylurea receptor SUR1. *J. Biol. Chem.* 272:22983–22986. doi:10.1074/jbc.272.37.22983

Xie, L.H., M. Takano, M. Kakei, M. Okamura, and A. Noma. 1999. Wortmannin, an inhibitor of phosphatidylinositol kinases, blocks the MgATP-dependent recovery of Kir6.2/SUR2A channels. *J. Physiol.* 514:655–665. doi:10.1111/j.1469-7793.1999.655ad.x

Zingman, L.V., A.E. Alekseev, M. Bienengraeber, D. Hodgson, A.B. Karger, P.P. Dzeja, and A. Terzic. 2001. Signaling in channel/enzyme multimers: ATPase transitions in SUR module gate ATP-sensitive K^+ conductance. *Neuron.* 31:233–245. doi:10.1016/S0896-6273(01)00356-7